Human Molecular Genetics, 2006, Vol. 15, No. 10 **1600–1609**
doi:10.1093/hmg/ddl081
Advance Access published on March 29, 2006

WFS1-deficiency increases endoplasmic reticulum stress, impairs cell cycle progression and triggers the apoptotic pathway specifically in pancreatic β-cells

Takahiro Yamada[1], Hisamitsu Ishihara[1,*], Akira Tamura[1], Rui Takahashi[1], Suguru Yamaguchi[1], Daisuke Takei[1], Ai Tokita[1], Chihiro Satake[1], Fumi Tashiro[3], Hideki Katagiri[2], Hiroyuki Aburatani[4], Jun-ichi Miyazaki[3] and Yoshitomo Oka[1]

[1]Division of Molecular Metabolism and Diabetes and [2]Division of Advanced Therapeutics for Metabolic Diseases, Tohoku University Graduate School of Medicine, 2-1 Seiryo-machi, Aoba-ku, Sendai, Miyagi 980-8575, Japan, [3]Division of Stem Cell Regulation Research, Osaka University Graduate School of Medicine, Suita, Osaka 565-0871, Japan and [4]Genome Science Division, Research Center for Advanced Science and Technology, The University of Tokyo, Tokyo 153-8904, Japan

Received January 28, 2006; Revised and Accepted March 24, 2006

Wolfram syndrome, an autosomal recessive disorder associated with diabetes mellitus and optic atrophy, is caused by mutations in the *WFS1* gene encoding an endoplasmic reticulum (ER) membrane protein. Herein, we report that pancreatic islets of *wfs1*-deficient mice exhibit increases in phosphorylation of RNA-dependent protein kinase-like ER kinase, chaperone gene expressions and active XBP1 protein levels, indicating an enhanced ER stress response. We established *wfs1*-deficient MIN6 clonal β-cells by crossing *wfs1*-deficient mice with mice expressing simian virus 40 large T antigen in β-cells. These cells show essentially the same alterations in ER stress responses as *wfs1*-deficient islets, which were reversed by re-expression of WFS1 protein or overexpression of GRP78, a master regulator of the ER stress response. In contrast, these changes are not observed in heart, skeletal muscle or brown adipose tissues with WFS1-deficiency. The increased ER stress response was accompanied by reduced BrdU incorporation and increased caspase-3 cleavage, indicating impaired cell cycle progression and accelerated apoptotic processes in the mutant islets. These changes are associated with increased expression of the cell cycle regulator $p21^{CIP1}$ in *wfs1*-deficient islets and clonal β-cells. Treatment of islets with thapsigargin, an ER stress inducer, caused upregulation of $p21^{CIP1}$. In addition, forced expression of $p21^{CIP1}$ resulted in reduced MIN6 β-cell numbers, suggesting the ER stress-induced increase in $p21^{CIP1}$ expression to be involved in β-cell loss in the mutant islets. These data indicate that WFS1-deficiency activates the ER stress response specifically in β-cells, causing β-cell loss through impaired cell cycle progression and increased apoptosis.

INTRODUCTION

Type 2 diabetes is caused by complex interactions between insulin resistance in peripheral tissues and impaired insulin secretion from pancreatic β-cells. There is a general consensus that the latter results from both impaired β-cell function and decreased β-cell mass (1–3). Adult β-cell mass is maintained by a balance between generation and death of β-cells. In patients with type 2 diabetes, new islet formation and β-cell replication are reportedly normal, and an increased rate of apoptosis has been suggested to underlie the loss of β-cell mass (4).

Recent studies using novel mutant mice have led to new insights into endoplasmic reticulum (ER) stress and maintenance

*To whom correspondence should be addressed. Tel: +81 227177611; Fax: +81 227177612; Email: hisamitsu-ishihara@mail.tains.tohoku.ac.jp

of β-cell mass (5,6). The ER stress response, also known as the unfolded protein response (UPR), involves translational attenuation, transcriptional induction of chaperones and folding enzymes, as well as degradation of misfolded proteins, a process called ER-associated degradation (ERAD). When ER stress is strong and cellular survival mechanisms fail to correct the protein-folding defects, an ER stress-mediated apoptotic process is initiated (5–7). Mice with a homozygous null mutation of RNA-dependent protein kinase-like ER kinase (PERK) lose their ability to phosphorylate eukaryotic initiation factor 2α (eIF2α) and fail to attenuate translation in response to ER stress. These mice develop diabetes owing to reduced β-cell mass (8). Importantly, mutations of the *EIF2AK3* gene encoding PERK in humans have been recognized as causing Wolcott-Rallison syndrome with diabetes mellitus in early infancy (9). A mouse model in which a Ser51Ala mutation of eIF2α prevents the protein from being phosphorylated by PERK and other eIF2α kinases, also displays a β-cell defect and impaired gluconeogenesis leading to lethal hypoglycemia (10). Mice with a deletion mutation of $P58^{IPK}$, a cytosolic chaperone, were recently reported to exhibit β-cell failure and diabetes (11). These examples suggest that β-cells, producing large quantities of insulin and thus a greater load on the ER, are especially sensitive to ER stress.

Wolfram syndrome is a rare autosomal recessive disorder characterized by juvenile-onset diabetes mellitus, optic atrophy, diabetes insipidus and sensorineural deafness (12). This syndrome is caused by mutations in the *WFS1* gene (13,14), which encodes an ER resident membrane protein (15). Post-mortem studies of the pancreas from subjects with Wolfram syndrome have shown β-cell loss (16). We recently established a line of mutant mice with a disrupted *wfs1* gene and found that these mice also exhibited impaired glucose homeostasis accompanied by a progressive reduction of β-cell mass (17). Thus, the *wfs1*-deficient mouse is a model for studying mechanisms of β-cell loss during the development of diabetes in Wolfram syndrome. We and others have also shown expression of WFS1 protein to be up-regulated by ER stress-inducing agents (18–20). A recent study employing IRE1α knockout and PERK knockout cells suggested that WFS1 is a component of the IRE1 and PERK signaling pathways (20). In addition, *wfs1*-deficient islets have been shown to exhibit increased DNA fragmentation in response to ER stress inducers (17), suggesting β-cell loss in Wolfram syndrome to be attributable to an inability to handle ER stress. A very recent study of islets conditionally lacking the *wfs1* gene in β-cells, demonstrated an increased GRP78 mRNA to GLUT2 mRNA ratio. This observation was interpreted as evidence of an enhanced ER stress response, on the assumption that GLUT2 mRNA levels represented the β-cell number in islets (21).

To further investigate the mechanisms underlying β-cell loss in Wolfram syndrome, we conducted a systematic study of the UPR in *wfs1*-deficient islets as well as other tissues. We also created β-cell lines with WFS1-deficiency and studied UPR. We found all three UPR subpathways to be activated in *wfs1*-deficient islets and β-cell lines. Furthermore, we demonstrated increased cleavage of caspase-3, a hallmark of apoptosis, and impaired proliferation associated with enhanced expression of the cell cycle regulator $p21^{CIP1}$.

RESULTS

UPR activation in *wfs1*-deficient islets

A systematic study of the UPR was conducted using islets isolated from 6-week-old male *wfs1*-deficient mice with the C57Bl/6 background. At 6 weeks of age, the β-cell mass of these mice begins to decrease (17). Accumulation of unfolded proteins in the ER is well known to induce dissociation of GRP78 from PERK, resulting in oligomerization and subsequent auto-phosphorylation of PERK. Activated PERK then phosphorylates eIF2α and suppresses general protein translation to reduce the ER load (5–7). In freshly isolated *wfs1*-deficient islets, PERK phosphorylation was increased (Fig. 1A). In addition, eIF2α phosphorylation was slightly but significantly enhanced with no alteration in total eIF2α levels in mutant islets (Fig. 1A). Thus, the ratio of phosphorylated eIF2α over total eIF2α levels analyzed by densitometry was increased by $27 \pm 7\%$ ($n = 4$ experiments, $P < 0.05$). These data indicate that one of three subpathways of the UPR arising from PERK phosphorylation is initiated in response to WFS1-deficiency in islets.

ER stress is also sensed by other ER resident proteins, IRE1 and ATF6, in addition to PERK (5–7). Activation of ATF6 via GRP78 dissociation and subsequent cleavage is known to induce the expressions of various chaperone genes, constituting another subpathway of the UPR (5–7). In *wfs1*-deficient islets, GRP94 mRNA levels were increased and those of GRP78 and $P58^{IPK}$ also tended to rise (Fig. 1B). Correspondingly, although the differences failed to reach statistical significance, levels of these chaperone proteins tended to be increased (Fig. 1C), suggesting that the ATF6 subpathway of the UPR is activated in response to WFS1-deficiency.

As shown in Figure 1D, a shorter form of XBP1 mRNA was increased. This form is produced by 26-nucleotide splicing from primary XBP1 mRNA by the ribonuclease activity of IRE1, increasing active XBP1 protein levels in mutant islets (Fig. 1E). HRD1, a ubiquitin ligase involved in ERAD, is one of the XBP1 target genes (22). In *wfs1*-deficient islets, levels of HRD1 protein were markedly increased (Fig. 1E). In addition, mRNA levels of ER-associated degradation-enhancing α-mannosidase-like protein (EDEM) (23), another target of XBP1, were significantly increased in mutant islets [100 ± 5 arbitrary units (wild-type) versus 136 ± 18 (mutant), $n = 6$, $P < 0.05$]. These data indicate that the IRE1-initiated subpathway of the UPR is also activated in *wfs1*-deficient islets.

Establishment of MIN6 β-cell lines deficient in WFS1

To examine the influence of WFS1-deficiency specifically in a homogenous β-cell population, β-cell lines were established by crossing $wfs1^{+/-}$ and $wfs1^{-/-}$ mice (17) with IT6 mice expressing simian virus 40 (SV40) large T antigen under the insulin promoter (24) and were designated MIN6wfs1$^{+/-}$ and MIN6wfs1$^{-/-}$, respectively (see Materials and Methods). IT6 mice were previously reported to develop insulinoma, from which the MIN6 cell line (24), one of the most highly differentiated β-cell lines, was generated. We established two cell lines each for the $wfs1^{+/-}$ and $wfs1^{-/-}$ genotypes. As shown in Figure 2A, the two cell lines with the $wfs1^{-/-}$ genotype (MIN6wfs1$^{-/-}$ – 1 and 2) show similar UPR

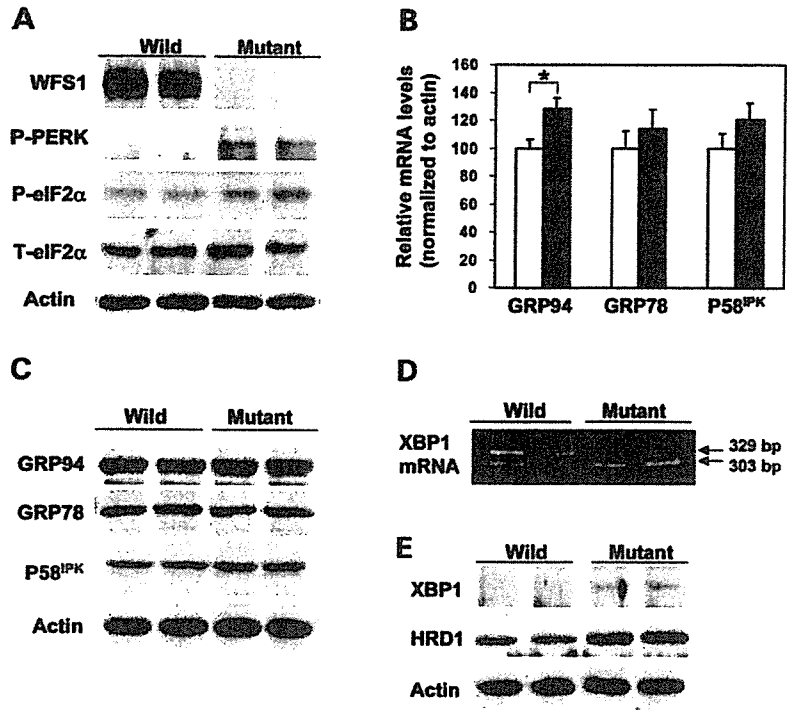

Figure 1. Activation of three subpathways of the UPR in *wfs1*-deficient islets. (**A**) Activation of the PERK/eIF2α pathway. Islets isolated from wild-type and *wfs1*-deficient mice were subjected to SDS–PAGE and probed with the indicated antibodies: P-PERK, phosphorylated-PERK; P-eIF2α, phosphorylated-eIF2α; T-eIF2α, total eIF2α. (**B**) Real-time RT–PCR analysis of GRP94, GRP78 and $P58^{IPK}$ gene expressions in wild-type (open columns) and *wfs1*-deficient (closed columns) mice. Relative mRNA levels were obtained after normalization to actin mRNA. $^{*}P < 0.05$, $n = 6$. (**C**) Expressions of chaperone proteins in *wfs1*-deficient islets. Lysates of isolated islets were probed with the indicated antibodies. (**D**) Increased XBP1 mRNA splicing in *wfs1*-deficient islets. Amplification of XBP1 mRNA from islet total RNA with specific primers yields spliced (303 bp) and non-spliced (329 bp) XBP1 transcripts. (**E**) Activation of the IRE1/XBP1 pathway. Lysates of isolated islets were probed with the indicated antibodies. Western blot data shown are representative of at least three experiments with different sets of samples.

characteristics. Similarly, characteristics of two cell lines with the *wfs1*$^{+/-}$ genotype (MIN6wfs1$^{+/-}$) were indistinguishable (data not shown). Therefore, only one line of each genotype was used for subsequent analyses. We compared MIN6wfs1$^{-/-}$ with MIN6wfs1$^{+/-}$ at the same passage numbers (passages 5–8), but not with the original MIN6 cells. This is because we were concerned that a difference in passage number between the original MIN6 and MIN6wfs1$^{-/-}$ cells, irrespective of WFS1-deficiency, might affect the protein expression profile, rendering the former an inappropriate control for the latter. After completion of a series of experiments, MIN6wfs1$^{+/-}$ cells reached passages 15–20, the same passage of original MIN6 cells we have. The function and survival of MIN6wfs1$^{+/-}$ cells are similar to those of wild-type MIN6 cells at similar passage numbers (data not shown).

Effects of WFS1-deficiency on UPR in β-cell lines

As shown in Figure 2A, altered expressions of UPR-related proteins observed in *wfs1*-deficient islets were reproduced in MIN6wfs1$^{-/-}$ cells; PERK phosphorylation, as well as expressions of active XBP1 and HRD1, were increased in *wfs1*-deficient MIN6 cells. ATF4 levels were also shown to be increased in these cells. Furthermore, although GRP78 and GRP94 protein levels were similar (Fig. 2B, upper panel), the activity of the GRP78 promoter containing three ER stress response elements was greater in MIN6wfs1$^{-/-}$ cells than in MIN6wfs1$^{+/-}$ cells (Fig. 2B), strongly suggesting activation of the ATF6 subpathway of the UPR in MIN6wfs1$^{-/-}$ cells. To confirm that alterations in UPR-related proteins are due to WFS1-deficiency, wild-type human WFS1 protein was expressed in MIN6wfs1$^{-/-}$ cells. We took advantage of the tetracycline-inducible expression system. MIN6wfs1$^{-/-}$ cells were infected with the Tet-repressor expressing virus (AdCAG-TR) together with a recombinant adenovirus bearing wild-type human WFS1 cDNA under the CMV promoter containing the Tet-operator (AdCTO-WFS1). The cells were then treated with doxycycline (2 μg/ml). As shown in Figure 2C, when WFS1 expression was restored to levels comparable to those of the original MIN6 cells, the increase in PERK phosphorylation was prevented. In addition, overexpression of GRP78, a master regulator of the ER stress response, also resulted in normalization of PERK phosphorylation levels (Fig. 2D), clearly indicating the observed alteration in UPR-related proteins to be due to exacerbation of ER stress caused by WFS1-deficiency.

No UPR induction in heart, skeletal muscle or brown adipose tissues from *wfs1*-deficient mice

WFS1 protein is expressed in a variety of non-pancreatic tissues, though less abundantly than in islets (Fig. 3A).

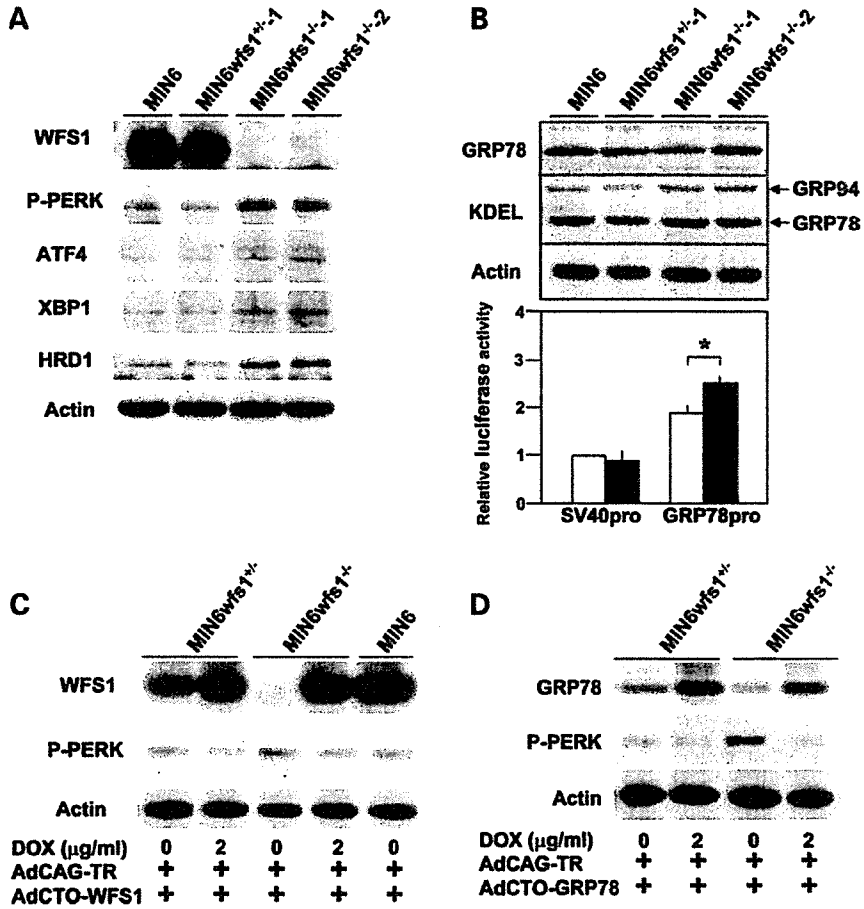

Figure 2. Increased UPR and its reversal by expression of WFS1 or GRP78 in an SV40 transformed *wfs1*-deficient β-cell line (MIN6wfs1$^{-/-}$). (**A**) Expression of UPR-related proteins in various MIN6 cell lines. MIN6, MIN6wfs1$^{+/-}$ − 1, MIN6wfs1$^{-/-}$ − 1 and MIN6wfs1$^{-/-}$ − 2 cells were lysed and probed with the indicated antibodies. Data shown are representative of at least three experiments with different sets of samples. (**B**) Expressions of chaperone proteins in MIN6wfs1$^{-/-}$ cells. (Upper panel) Cellular lysates were probed with anti-GRP78, anti-KDEL and anti-actin (loading control) antibodies. (Lower panel) MIN6wfs1$^{+/-}$ (open columns) and MIN6wfs1$^{-/-}$ (closed columns) cells were transiently transfected with the pGL3-promoter plasmid containing the SV40 promoter-luciferase (SV40pro: 0.5 μg) or pGRP78pro(−172)-Luc (GRP78pro: 0.5 μg) together with the reference plasmid pTK-RL (0.05 μg) encoding *Renilla* luciferase. Twenty-four hours after transfection, cellular lysates were subjected to luciferase assay. The luciferase activity of the pGL3-promoter in MIN6wfs1$^{+/-}$ was defined as 1. The averages of three independent experiments, each performed in duplicate, are presented. $^{*}P < 0.05$, $n = 3$. (**C**) Suppression of PERK phosphorylation by WFS1 re-expression in MIN6wfs1$^{-/-}$ cells. Cells were infected with AdCAG-TR expressing Tet-repressor and AdCTO-WFS1 harboring *WFS1* cDNA. WFS1 expression was induced by 48 h doxycycline (DOX, 2 μg/ml) treatment. The experiment was repeated three times and similar results were obtained. (**D**) Suppression of PERK phosphorylation by GRP78 overexpression in MIN6wfs1$^{-/-}$ cells. Human GRP78 expression was induced by 48 h DOX treatment. The experiment was repeated four times and similar results were obtained.

Therefore, we also examined expressions of UPR genes in tissues other than pancreatic islets. Cardiac function is reportedly not impaired in subjects with Wolfram syndrome (12) or in *wfs1*-deficient mice (17). Skeletal muscle and brown adipose tissue also appear essentially normal in mutant mice (data not shown). In contrast to islets, no UPR alterations were observed in these tissues from *wfs1*-deficient mice (Fig. 3B–D). Thus, UPR activation is tissue-specific in WFS1-deficiency.

Increased β-cell apoptotic response in *wfs1*-deficient islets

ER stress induces apoptosis through activation of various signaling molecules including JNK and pro-apoptotic proteins, such as CHOP (5–7). CHOP expression was increased at both the mRNA (Fig. 4A) and the protein level (Fig. 4B), in mutant when compared with wild-type islets. In contrast, JNK expression levels and phosphorylation states were not altered in *wfs1*-deficient islets (Fig. 4B). We also found increased levels of cleaved caspase-3, a hallmark of apoptosis, in mutant islets (Fig. 4B). CHOP expression and cleaved caspase-3 levels were also increased in *wfs1*-deficient MIN6 cells (Fig. 4C), whereas no such changes were observed in heart, skeletal muscle or adipose tissue (data not shown).

We also measured apoptosis in MIN6wfs1$^{-/-}$ and MIN6wfs1$^{+/-}$ cells by counting adherent cells positive for annexin V staining under fluorescent microscope. We found 1–2% cells to be annexin V positive for both the *wfs1*$^{-/-}$ and the *wfs1*$^{+/-}$ genotype cultured under standard conditions, i.e. no differences between MIN6wfs1$^{-/-}$ and MIN6wfs1$^{+/-}$

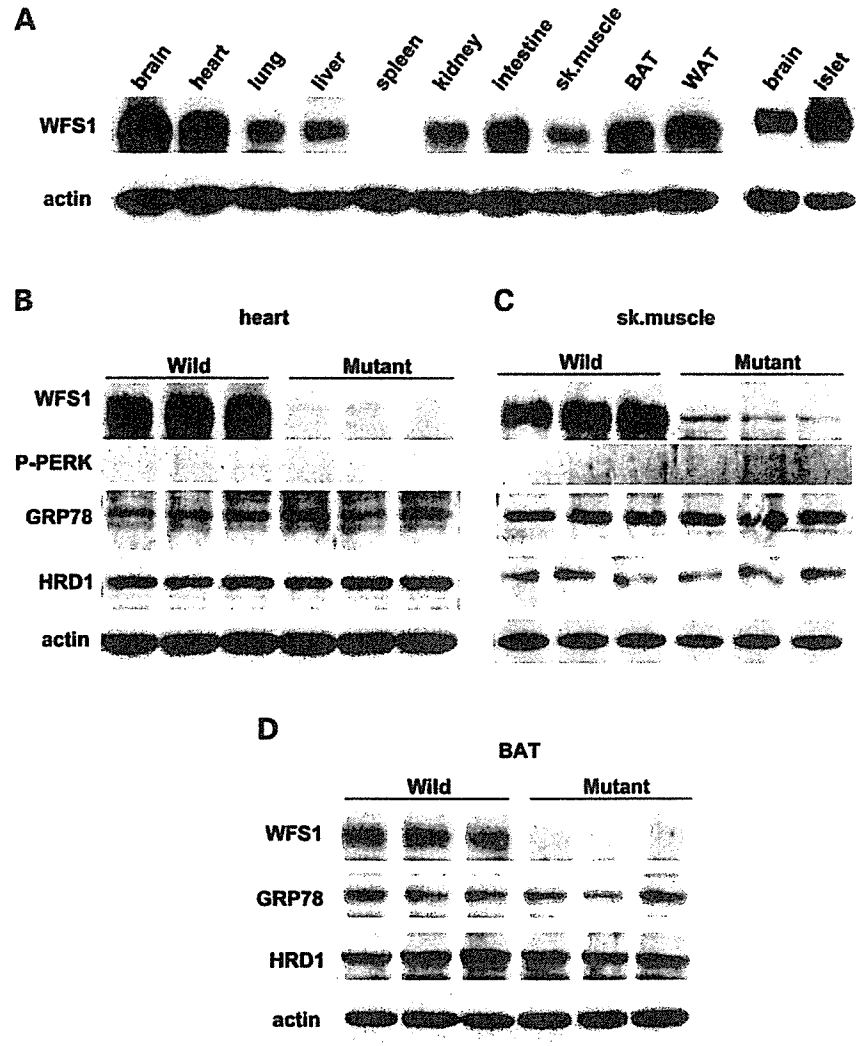

Figure 3. No UPR changes in heart, skeletal muscle or brown adipose tissue from *wfs1*-deficient mice. (A) WFS1 protein distribution in mice. Approximately, 100 μg of protein from wild-type mouse tissues were analyzed for the presence of WFS1 protein. BAT, brown adipose tissue; WAT, white adipose tissue. (**B–D**) UPR activation was not observed in heart (B), skeletal muscle (C) or BAT (D) from *wfs1*-deficient mice. The western blot data shown are representative of two experiments, each performed using three mice of each genotype.

cells. An increase in the number of apoptotic cells was observed when MIN6wfs1$^{-/-}$ cells were challenged with 0.5 μM thapsigargin (TG) for 24 h, as compared with MIN6wfs1$^{+/-}$ cells under the same conditions [2.7 ± 1.0% (MIN6wfs1$^{+/-}$) versus 6.2 ± 1.1% (MIN6wfs1$^{-/-}$) $n = 3$, $P < 0.05$]. Therefore, MIN6wfs1$^{-/-}$ cells exhibited increased apoptosis susceptibility. These data, together, indicate that an ER stress mediated-apoptotic process is activated in *wfs1*-deficient β-cells.

Impaired β-cell proliferation in *wfs1*-deficient islets

In addition to increased apoptosis, decreased proliferation may contribute to loss of β-cell mass in *wfs1*-deficient mice. When β-cell proliferation activity was assayed by 5-bromodeoxyuridine (BrdU) incorporation in pancreases from wild-type and mutant mice, BrdU incorporation was found to be significantly reduced in *wfs1*-deficient β-cells (Fig. 5A and B). This observation suggested impaired proliferation, along with increased apoptosis, to contribute to β-cell loss in *wfs1*-deficient islets.

We next explored possible causes of the decreased β-cell proliferation in *wfs1*-deficient islets. The link between the UPR and cell cycle arrest was previously reported to be mediated by down-regulation of cyclin D1 because of general translational suppression via eIF2α phosphorylation (25). However, neither expression of cyclin D1 nor that of cyclin D2, major isoforms of the D type cyclins in β-cells (26,27), was changed in mutant islets (data not shown). CHOP has also been recognized as causing cell cycle arrest and apoptosis (28,29). As GADD34 is reportedly a target of CHOP (30) and is involved in cell growth and survival (31),

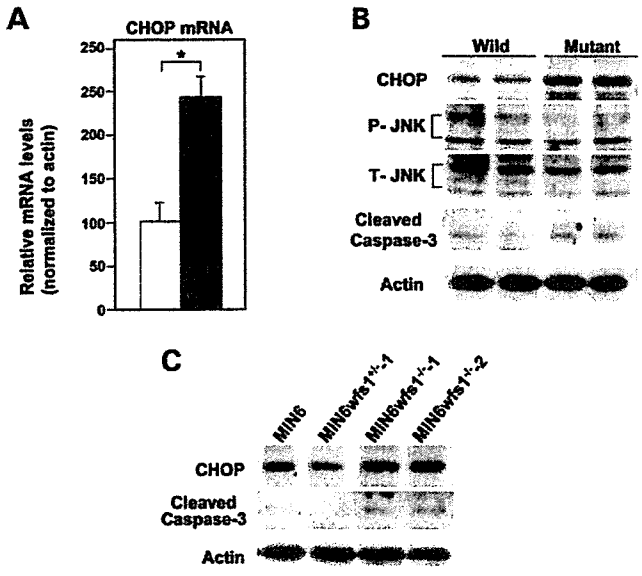

Figure 4. Activation of apoptosis signaling in *wfs1*-deficient islets and MIN6 cells. (**A**) Real-time RT–PCR analysis of CHOP mRNA in wild-type (open column) and *wfs1*-deficient (closed column) islets. Relative mRNA levels were obtained after normalization to actin mRNA. $^{*}P < 0.05$, $n = 6$. (**B**) Western blot analysis of apoptosis signaling proteins in *wfs1*-deficient islets. Lysates of islets were probed with the indicated antibodies: P-JNK, phospho-JNK; T-JNK, total-JNK. Data shown are representative of three experiments with different sets of samples. (**C**) Increased expression of CHOP and cleaved caspase-3 in *wfs1*-deficient MIN6 cells. Lysates of MIN6 cell derivatives were probed with the indicated antibodies. Data shown are representative of three experiments.

GADD34 expression was examined. GADD34 transcript levels were found to be increased in *wfs1*-deficient islets (100 ± 11 versus 151 ± 14, $P < 0.05$). Recent studies have demonstrated that cell cycle regulation is critical for maintenance of β-cell mass (25,26). As GADD34 reportedly induces p53 phosphorylation and enhances expression of the cell cycle inhibitor $p21^{CIP1}$ (32), p53 and $p21^{CIP1}$ expressions were assessed. We found phosphorylation of p53 to be increased, though total p53 was not elevated (Fig. 5C). In addition, increased expressions of $p21^{CIP1}$ mRNA (100 ± 11 versus 413 ± 32, $P < 0.01$) and $p21^{CIP1}$ protein (Fig. 5C) were observed in *wfs1*-deficient islets. We also examined the expression of another cell cycle inhibitor, $p27^{KIP1}$, and found no difference between wild-type and mutant islets (Fig. 5C). Increased expression of $p21^{CIP1}$ protein was also observed in *wfs1*-deficient MIN6 cells, SV40 large T antigen-transformed cells in which p53 activity was considered to be suppressed (Fig. 5D). Expression of $p21^{CIP1}$ protein was not increased in heart, skeletal muscle or brown adipose tissues from *wfs1*-deficient mice (data not shown).

In order to determine whether increased expression of $p21^{CIP1}$ is attributable to ER stress, wild-type islets were treated with TG (0.5 μM) for 12 h. As shown in Figure 5E, expression of $p21^{CIP1}$ was significantly increased. In addition, expression of $p21^{CIP1}$ was markedly increased in MIN6 cells treated with TG (Fig. 5F) or tunicamycin (data not shown). These data suggest 21^{CIP1} expression to be induced by ER stress in β-cells.

Finally to assess the effects of $p21^{CIP1}$ expression on β-cell proliferation, $p21^{CIP1}$ was expressed in wild-type MIN6 cells in a tetracycline-inducible manner (Fig. 6A). Overexpression of $p21^{CIP1}$ suppressed a MIN6 cell number increase (Fig. 6B), suggesting that increased $p21^{CIP1}$ expression contributes to the reduced β-cell mass in *wfs1*-deficient islets.

DISCUSSION

We systematically investigated UPR in *wfs1*-deficient islets and MIN6 β-cells as well as heart, skeletal muscle and brown adipose tissues from the mutant mice in this study. Enhanced UPR was specifically observed in β-cells but not in other tissues examined. These findings indicate that diabetes in Wolfram syndrome is caused by increased ER stress in β-cells and establish Wolfram syndrome as an ER stress-based disease, as is the case in Wolcott-Rallison syndrome with PERK-deficiency (9). Furthermore, we found enhanced UPR to be associated with not only activation of the apoptotic pathway but also impaired cell cycle progression in β-cells. These observations provide evidence of novel mechanisms underlying ER stress-mediated β-cell loss.

We demonstrated activation of the PERK and IRE1 subpathways of the UPR. Increased activation of the GRP78 promoter indicates the ATF6 subpathway to be induced as well. GRP78 expression was also reportedly increased by knockdown of WFS1 expression in INS1 insulinoma β-cells (20). Collectively, these data indicate that all three UPR subpathways are activated by WFS1-deficiency in β-cells. The UPR is activated when ER homeostasis is perturbed by defective ER calcium homeostasis, mutations in ER resident proteins and/or abnormalities of the ERAD system. Disturbed ER homeostasis is also induced by defect(s) in components of the UPR system, as is the case in Wolcott-Rallison syndrome with PERK-deficiency. The present data suggest that impaired ER homeostasis does not result from defect(s) in a specific pathway(s) of the UPR. Our previous study demonstrated an abnormal cytosolic Ca^{2+} response in *wfs1*-deficient β-cells (17), suggesting that impaired ER Ca^{2+} homeostasis is a possible cause of ER stress associated with WFS1-deficiency.

We found that WFS1 protein is highly expressed in heart, skeletal muscle and brown adipose tissues. However, there is no UPR activation in these tissues from mutant mice. Thus, the UPR is tissue-specific in *wfs1*-deficient mice. One possible explanation of this tissue specificity is that a protein(s), compensating for loss of WFS1 protein function is present in these tissues but not in β-cells. This interesting possibility merits further investigation and elucidation of WFS1 function is necessary to resolve the tissue-specific effects of WFS1-deficiency.

Our results demonstrate, in addition to the augmented apoptotic process evidenced by increased caspase-3 cleavage, that β-cell proliferation is decreased in *wfs1*-deficient mice. Impaired proliferation was also reported in BRIN-BD11 cells expressing the human WFS1 antisense transcript (33). Our observation is in contrast to that by Riggs *et al.* (21) who detected no changes in the numbers of BrdU-positive cells in islets from β-cell specific *wfs1* knockout mice. The reason for this discrepancy is currently unclear, but may

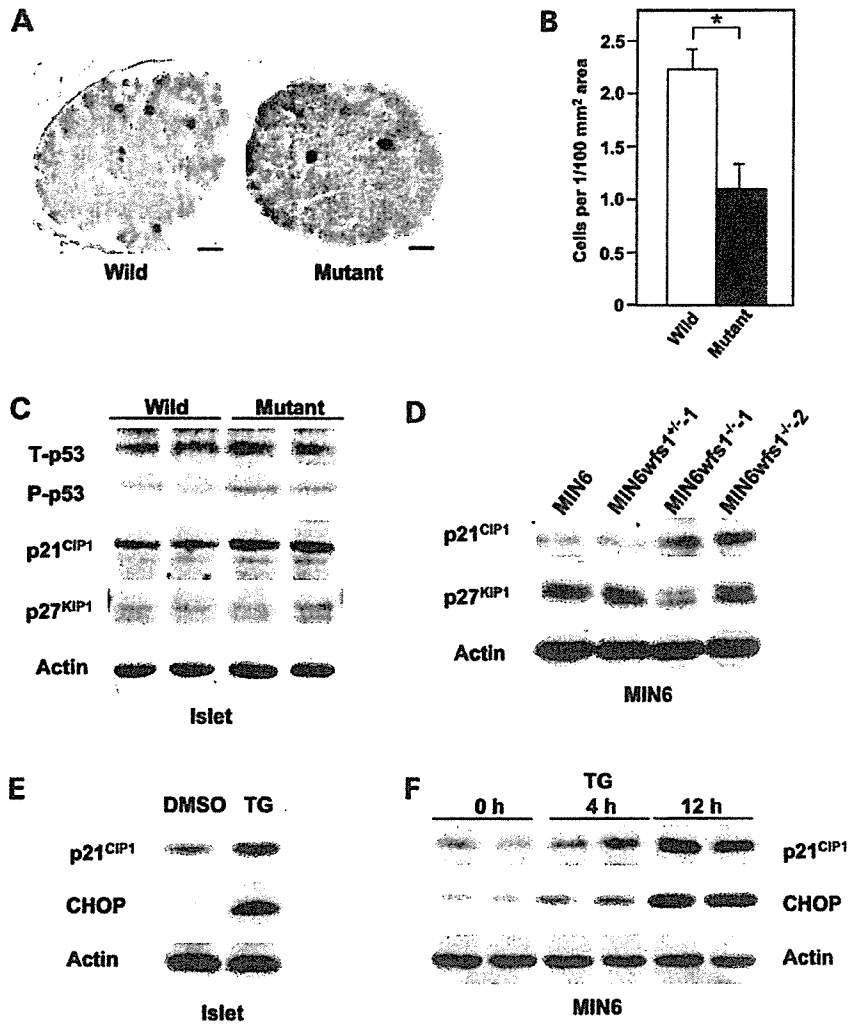

Figure 5. Impaired cell cycle progression and increased $p21^{CIP1}$ expression in *wfs1*-deficient islets. (**A** and **B**) Impaired cell cycle progression in *wfs1*-deficient β-cells. Incorporated BrdU and insulin were probed with specific antibodies (A) and BrdU positive β-cells were counted (B). Bars, 10 μM. $^*P < 0.05$, $n = 4$ mice per group. (**C** and **D**) Increased $p21^{CIP1}$ expression in *wfs1*-deficient islets and MIN6 cells. Lysates of wild-type and *wfs1*-deficient islets (C) or MIN6 cells (D) were probed with the indicated antibodies: T-p53, total-p53; P-p53, phospho-p53. Data shown are representative of three experiments with different sets of samples. (**E** and **F**) Induction of $p21^{CIP1}$ expression by TG in islets (E) and MIN6 cells (F). Wild-type islets were challenged with 0.5 μM TG for 12 h. MIN6 cells were also treated with 0.5 μM TG for the indicated durations. Lysates of islets or MIN6 cells were probed with the indicated antibodies. The experiment was repeated three times and similar results were obtained.

reflect differences in the ages of the mice studied: 6-week-old mice were used in the present versus 12- or 24-week-old animals in their study (21). Cell cycle dysregulation in *wfs1*-deficient islets was associated with increased expression of $p21^{CIP1}$, a cell cycle regulator. $p21^{CIP1}$ can serve, depending on which tissues or cells it is activated in, as both an inhibitor and an agonist of cell cycle progression (34). Our observation that forced expression of $p21^{CIP1}$ suppressed MIN6 β-cell proliferation suggests that $p21^{CIP1}$ operates as a cell cycle inhibitor in β-cells, although our results must be interpreted cautiously, as forced overexpression of $p21^{CIP1}$ may produce effects different from those occurring in mutant β-cells with increased $p21^{CIP1}$ levels. A very recent study, demonstrating that $p21^{CIP1}$ acts as a molecular brake on mitogenic stimuli in β-cells (35), supports the notion of $p21^{CIP1}$ functioning as a cell cycle inhibitor in β-cells. ER stress inducers were recently reported to cause $p21^{CIP1}$ expression and cell cycle arrest in chondrocytes (36) and prostatic cancer cells (37), suggesting that cell cycle arrest associated with increased $p21^{CIP1}$ expression is a common feature in cells under ER stress. Furthermore, reduced proliferation associated with increased expression of $p21^{CIP1}$, in *wfs1*-deficient β-cells (the present study) and β-cells transgenic for hepatocyte growth factor and/or placental lactogen (35), highlights an important role for $p21^{CIP1}$ in regulation of β-cell mass in addition to the roles of $p27^{KIP1}$ recently reported (38).

CHOP induces GADD34 expression (30), which then activates p53 phosphorylation and $p21^{CIP1}$ transcription (32). Therefore, the CHOP → GADD34 → p53 pathway is a candidate for ER stress-mediated $p21^{CIP1}$ expression. Indeed,

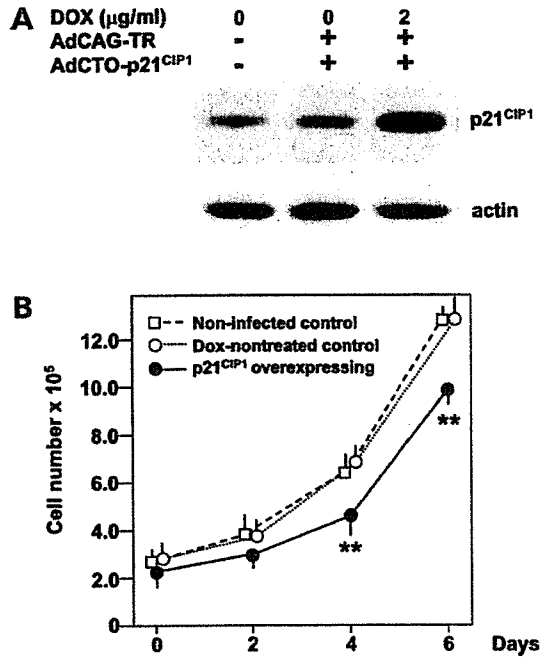

Figure 6. Decrease in MIN6 cell numbers in response to forced $p21^{CIP1}$ expression. (A) Forced expression of $p21^{CIP1}$ in MIN6 cells. Cells were either uninfected or infected with AdCAG-TR (m.o.i. of 30) and AdCTO-$p21^{CIP1}$ (m.o.i. of 100) harboring $p21^{CIP1}$ cDNA. Expression of $p21^{CIP1}$ was induced by 48 h DOX (2 μg/ml) treatment. MIN6 cell lysates were subjected to immunoblot analysis using anti-$p21^{CIP1}$ and actin antibodies. (B) Numbers of MIN6 cells overexpressing $p21^{CIP1}$. One day after adenovirus transduction, cells were reseeded (2×10^5 per well) and divided into two groups, and, after two more days, treatment with (closed circles) or without (open circles) DOX (2 μg/ml) was commenced (day 0). Uninfected MIN6 cells (open squares) were also seeded 2 days before. Cells were then harvested on days 0, 2, 4 and 6, stained with trypan blue and counted. Data are means ± S.E. for triplicate wells. $^{**}P < 0.01$ against both controls. The experiment was repeated three times and similar results were obtained.

an increase in $p21^{CIP1}$ expression was associated with increased GADD34 expression and p53 phosphorylation in *wfs1*-deficient β-cells. However, induction of $p21^{CIP1}$ expression by TG was observed in MIN6 cells transformed with SV40 large T antigen, a well-known suppressor of p53. In addition, an ER stress-induced increase in $p21^{CIP1}$ expression was observed in p53-deficient prostatic cancer cells (37). Thus, ER stress appears to induce $p21^{CIP1}$ expression through both p53-dependent and -independent mechanisms.

As β-cells are apparently much more sensitive to ER stress than other types of cells and tissues (39), ER stress might be a more common cause of β-cell failure than previously thought, especially in terms of the increased insulin demands of modern lifestyles. Our data indicate that both increased apoptosis and impaired proliferation, in β-cells, are mechanisms leading to β-cell loss in *wfs1*-deficient islets, a model of ER-stress mediated β-cell failure. Further studies designed to elucidate the molecular mechanisms of β-cell loss under chronic ER stress are anticipated to contribute to future treatments for type 2 diabetes.

MATERIALS AND METHODS

Antibodies

The monoclonal antibody against $P58^{IPK}$ was a generous gift from Prof. M.G. Katze (University of Washington). Other antibodies were purchased from the indicated sources: anti-GRP94, anti-KDEL (Stressgen Biotechnologies), anti-GRP78, anti-XBP1, anti-$p21^{CIP1}$, anti-CHOP, anti-p53, anti-phosphorylated p53 and anti-ATF4 (Santa Cruz Biotechnology), anti-HRD1 (Abgent), anti-phosphorylated PERK, anti-JNK, anti-phosphorylated JNK, anti-eIF2α, anti-phosphorylated eIF2α, and anti-cleaved caspase-3 (Cell Signaling), and anti-$p27^{KIP1}$ (BD Transduction Laboratories).

Mouse islet isolation, real-time RT–PCR and western blot

The *wfs1*-deficient mice used had a C57Bl/6 background and were described previously (17). All animal experiments were approved by the Tohoku University Institutional Animal Care and Use Committee (#15–45). Islets were isolated by collagenase infusion through the common bile duct and harvested by hand. Total RNA was prepared immediately after islet isolation using an RNAeasy kit (Qiagen). For real-time RT–PCR analysis, cDNA was synthesized by reverse transcription using the oligo $d(T)_{16}$ primer and subjected to PCR amplification with gene-specific primers (Table 1) using a SYBR Green 1 kit (Roche). Data are presented as relative values to actin mRNA. For detection of the spliced form of XBP1 mRNA, the primers were: 5′-TGAGAACCAGGA GTTAAGAAACGC-3′ and 5′-TTCTGGGTAGACCTCTGG GAGTTCC-3′. For immunoblotting, islets from three to four mice were pooled, dissolved immediately after isolation in a lysis buffer (~100 islets/15 μl) and subjected to SDS–polyacrylamide gel electrophoresis. In several experiments, isolated islets were cultured overnight and treated with 0.5 μM TG for 12 h. All western blot experiments were repeated at least three times, with different sets of samples, throughout this study. Immunoblot band intensities were analyzed using Scion image software (Scion Corporation) and normalized with those of actin.

Establishment of MIN6wfs1$^{-/-}$ and MIN6wfs1$^{+/-}$ cell lines

The *wfs1*$^{-/-}$ mice (17) were bred with IT6 mice expressing SV40 large T antigen under the human insulin promoter (24) and the resulting *wfs1*$^{+/-}$:SV40Tag/+ mice were further bred with *wfs1*$^{-/-}$ mice. Tumors from pancreases of 10- to 12-week-old *wfs1*$^{+/-}$:SV40Tag/+ and *wfs1*$^{-/-}$: SV40Tag/+ mice were carefully excised and placed in Dulbecco's Modified Eagle's Medium containing penicillin and streptomycin. Cells were expanded and frozen at passages 3 and 4. We used these cells at 5–8 passages in this study. For study of apoptosis, MIN6 cells were infected with AdRIPeGFP expressing enhanced green fluorescent protein under the insulin promoter to facilitate detection of cells under fluorescent microscope. Apoptosis was examined by staining with annexin V using the Annexin V-Cy3 apoptosis detection kit

Table 1. Primers used for quantitative real-time RT–PCR

Genes	Forward	Reverse
ATF4	5′-TCCTGAACAGCGAAGTGTTG-3′	5′-ACCCATGAGGTTTCAAGTGC-3′
GRP94	5′-TGATGAAGTCGACGTGGATG-3′	5′-TCCTGTTCACTTCAGCTTGG-3′
GRP78	5′-GACATTTGCCCAGAAGAAA-3′	5′-CTCATGACATTCAGTCCAGCA-3′
P58^{IPK}	5′-CCTTATCGGACAGTCCTTCG-3′	5′-TCAGAGTCCTGATTTCATCTTCA-3′
EDEM	5′-GGAAATTCATCCGAGTTCCA-3′	5′-GGGCCATGTACAACAATTCA-3′
CHOP	5′-CCTAGCTTGGCTGACAGAGG-3′	5′-CTGCTCCTTCTCCTTCATGC-3′
GADD34	5′-CGGAGAGAAGCCAGAATCAC-3′	5′-CAGCAAGGAAATGGACTGTG-3′
P21^{CIP1}	5′-ACATCTCAGGGCCGAAAAC-3′	5′-CCTGACCCACAGCAGAAGAG-3′

(Medical and Biological Laboratories). At least 1000 cells per sample were counted for annexin V positive cells.

GRP78 promoter assay

The pGL3-promoter, pTK-RLuc and pGL3-basic plasmids were purchased from Promega. The mouse GRP78 promoter fragment spanning −172 to −21 (positions relative to the transcription start site) was amplified by PCR using oligonucleotides 5′-GACTCGAGGCCGCTTCGAATCGGCAG-3′ and 5′-TCAAGCTTGGCCAGTATCGAGCGCGC-3′. This fragment contains three ER stress response elements (40) and the corresponding regions of human (40) and rat (41) *GRP78* genes were shown to respond to ATF6 activation. A GRP78 promoter-driving luciferase reporter plasmid (designated pmGRP78pro(−172)-Luc) was constructed by subcloning this fragment into the *Xho*I and *Hind*III sites of the pGL3-basic vector. MIN6wfs1$^{+/-}$ or MIN6wfs1$^{-/-}$ cells were co-transfected with pGL3-promoter or pGRP78pro(−172)-Luc together with pTK-RLuc using the LipofectAMINE reagent (Invitrogen). Luciferase activities were assayed with Dual-Luciferase reporter system (Promega) using a Lumat LB9507 luminometer (Berthold).

BrdU incorporation assay

BrdU (100 mg/kg) was injected into the mice intraperitoneally. Six hours later, the mice were sacrificed and their pancreases were fixed with 4% paraformaldehyde. Immunohistochemical analyses were performed with a Cell Proliferation Assay kit (BD Pharmingen). Sections were also stained with anti-insulin. BrdU-positive β-cells were counted in at least 50 sections per mouse.

Recombinant adenovirus experiments

Human *GRP78* cDNA was purchased from Open Biosystems. Human *WFS1* cDNA was a generous gift from Prof. Y. Tanizawa (Yamaguchi University). The CMV promoter containing two Tet-operator sequences (designated CTO) was excised from pcDNA5/TO (Invitrogen) and ligated to these cDNAs. The Tet-repressor cDNA was excised from pcDNA6/TR (Invitrogen) and ligated to the CAG promoter unit (42). These expression units were used to generate recombinant adenoviruses by a previously described method (43). The resulting viruses were designated AdCAG-TR for the Tet-repressor expressing virus and AdCTO-GRP78 for the GRP78 expressing virus under the CTO promoter, and so on. MIN6 and its derivative cells were infected with AdCAG-TR at a multiplicity of infection (m.o.i.) of 30 together with viruses with the CTO promoter at an m.o.i. of 100. One day after infection, cells were reseeded and divided into two groups. Two days thereafter, the cells were fed media with or without doxycycline (2 μg/ml). We have observed no adverse effects of infection of a control recombinant adenovirus expressing green fluorescence protein at an m.o.i. of less than 250 on MIN6 cell function in terms of cell proliferation and glucose-stimulated insulin secretion (data not shown). For the cell number assessment, MIN6 cells infected with AdCAG-TR and AdCTO-p21^{CIP1} were seeded in six-well plates at 2×10^5 per well, cultured in media with or without doxycycline (2 μg/ml) and harvested after the indicated intervals. Cells were then stained with trypan blue and counted.

Statistical analysis

Data are presented as means ± S.E. Differences between groups were assessed by Student's *t*-test.

ACKNOWLEDGEMENTS

We thank Profs. M.G. Katze and Y. Tanizawa for their generous gifts of the monoclonal antibody against P58^{IPK} and human WFS1 cDNA, respectively. We are also grateful to Y. Nagura and K. Tanaka for their expert assistance. This research was supported by Grants-in-Aid for Scientific Research (17590264 to H.I. and 17390258 to Y.O.) from the Ministry of Education, Science, Sports and Culture of Japan.

Conflict of Interest statement. None declared.

REFERENCES

1. Donath, M.Y. and Halban, P.A. (2004) Decreased beta-cell mass in diabetes: significance, mechanisms and therapeutic implications. *Diabetologia*, **47**, 581–589.
2. Rhodes, C.J. (2005) Type 2 diabetes–a matter of beta-cell life and death? *Science*, **307**, 380–384.
3. Porter, J.R. and Barrett, T.G. (2005) Monogenic syndromes of abnormal glucose homeostasis: clinical review and relevance to the understanding of the pathology of insulin resistance and beta cell failure. *J. Med. Genet.*, **42**, 893–902.
4. Butler, A.E., Janson, J., Bonner-Weir, S., Ritzel, R., Rizza, R.A. and Butler, P.C. (2003) Beta-cell deficit and increased beta-cell apoptosis in humans with type 2 diabetes. *Diabetes*, **52**, 102–110.

5. Harding, H.P. and Ron, D. (2002) Endoplasmic reticulum stress and the development of diabetes: a review. *Diabetes*, **51** (Suppl. 3), S455–S461.
6. Wu, J. and Kaufman, R.J. (2006) From acute ER stress to physiological roles of the unfolded protein response. *Cell Death Differ.*, **13**, 374–384.
7. Schroder, M. and Kaufman, R.J. (2005) The mammalian unfolded protein response. *Annu. Rev. Biochem.*, **74**, 739–789.
8. Harding, H.P., Zhang, Y., Zeng, H., Jungries, R., Chung, P., Plesken, H., Sabatini, D.D. and Ron, D. (2001) Diabetes mellitus and exocrine pancreatic dysfunction in perk−/− mice reveals a role for translational control in secretory cell survival. *Mol. Cell*, **7**, 1153–1163.
9. Delepine, M., Nicolino, M., Barrett, T., Golamaully, M., Lathrop, G.M. and Julier, C. (2000) *EIF2AK3*, encoding translation initiation factor 2-alpha kinase 3, is mutated in patients with Wolcott-Rallison syndrome. *Nat. Genet.*, **25**, 406–409.
10. Scheuner, D., Song, B., McEwen, E., Liu, C., Laybutt, R., Gillespie, P., Saunders, T., Bonner-Weir, S. and Kaufman, R.J. (2001) Translational control is required for the unfolded protein response and *in vivo* glucose homeostasis. *Mol. Cell*, **7**, 1165–1176.
11. Ladiges, W.C., Knoblaugh, S.E., Morton, J.F., Korth, M.J., Sopher, B.L., Baskin, C.R., MacAuley, A., Goodman, A.G., LeBoeuf, R.C. and Katze, M.G. (2005) Pancreatic β-cell failure and diabetes in mice with a deletion mutation of the endoplasmic reticulum molecular chaperone gene $P58^{IPK}$. *Diabetes*, **54**, 1074–1081.
12. Wolfram, D.J. and Wagener, H.P. (1938) Diabetes mellitus and simple optic atrophy among siblings: report on four cases. *Mayo Clinic Proc.*, **13**, 715–718.
13. Inoue, H., Tanizawa, Y., Wasson, J., Behn, P., Kalidas, K., Bernal-Mizrachi, E., Mueckler, M., Marshall, H., Donis-Keller, H., Crock, P. *et al.* (1998) A gene encoding a transmembrane protein is mutated in patients with diabetes mellitus and optic atrophy (Wolfram syndrome). *Nat. Genet.*, **20**, 143–148.
14. Strom, T.M., Hortnagel, K., Hofmann, S., Gekeler, F., Scharfe, C., Rabl, W., Gerbitz, K.D. and Meitinger, T. (1998) Diabetes insipidus, diabetes mellitus, optic atrophy and deafness (DIDMOAD) caused by mutations in a novel gene (wolframin) coding for a predicted transmembrane protein. *Hum. Mol. Genet.*, **7**, 2021–2028.
15. Takeda, K., Inoue, H., Tanizawa, Y., Matsuzaki, Y., Oba, J., Watanabe, Y., Shinoda, K. and Oka, Y. (2001) *WFS1* (Wolfram syndrome 1) gene product: predominant subcellular localization to endoplasmic reticulum in cultured cells and neuronal expression in rat brain. *Hum. Mol. Genet.*, **10**, 477–484.
16. Karasik, A., O'hara, C., Srikanta, S., Swift, M., Soeldner, J.S., Kahn, C.R. and Herskowitz, R.D. (1989) Genetically programmed selective islet beta-cell loss in diabetic subjects with Wolfram's syndrome. *Diab. Care*, **12**, 135–138.
17. Ishihara, H., Takeda, S., Tamura, A., Takahashi, R., Yamaguchi, S., Takei, D., Yamada, T., Inoue, H., Soga, H., Katagiri, H. *et al.* (2004) Disruption of the *wfs1* gene in mice causes progressive beta-cell loss and impaired stimulus-secretion coupling in insulin secretion. *Hum. Mol. Genet.*, **13**, 1159–1170.
18. Yamaguchi, S., Ishihara, H., Tamura, A., Yamada, T., Takahashi, R., Takei, D., Katagiri, H. and Oka, Y. (2004) Endoplasmic reticulum stress and *N*-glycosylation modulate expression of WFS1 protein. *Biochem. Biophys. Res. Commun.*, **325**, 250–256.
19. Ueda, K., Kawano, J., Takeda, K., Yujiri, T., Tanabe, K., Anno, T., Akiyama, M., Nozaki, J., Yoshinaga, T., Koizumi, A. *et al.* (2005) Endoplasmic reticulum stress induces *Wfs1* gene expression in pancreatic β cells via transcriptional activation. *Eur. J. Endocr.*, **153**, 167–176.
20. Fonseca, S.G., Fukuma, M., Lipson, K.L., Nguyen, L.X., Allen, J.R., Oka, Y. and Urano, F. (2005) WFS1 is a novel component of the unfolded protein response and maintains homeostasis of the endoplasmic reticulum in pancreatic β-cells. *J. Biol. Chem.*, **280**, 39609–39615.
21. Riggs, A.C., Bernal-Mizrachi, E., Ohsugi, M., Wasson, J., Fatrai, S., Welling, C., Murray, J., Schmidt, R.E., Herrera, P.L. and Permutt, M.A. (2005) Mice conditionally lacking the Wolfram gene in pancreatic islet beta cells exhibit diabetes as a result of enhanced endoplasmic reticulum stress and apoptosis. *Diabetologia*, **48**, 2313–2321.
22. Kaneko, M., Ishiguro, M., Niinuma, Y., Uesugi, M. and Nomura, Y. (2002) Human HRD1 protects against ER stress-induced apoptosis through ER-associated degradation. *FEBS Lett.*, **532**, 147–152.
23. Hosokawa, N., Wada, I., Hasegawa, K., Yorihuzi, T., Tremblay, L.O., Herscovics, A. and Nagata, K. (2001) A novel ER alpha-mannosidase-like protein accelerates ER-associated degradation. *EMBO Rep.*, **2**, 415–422.
24. Miyazaki, J., Araki, K., Yamato, E., Ikegami, H., Asano, T., Shibasaki, Y., Oka, Y. and Yamamura, K. (1990) Establishment of a pancreatic β cell line that retains glucose-inducible insulin secretion: special reference to expression of glucose transporter isoforms. *Endocrinology*, **127**, 126–132.
25. Brewer, J.W. and Diehl, J.A. (2000) PERK mediates cell-cycle exit during the mammalian unfolded protein response. *Proc. Natl Acad. Sci. USA*, **97**, 12625–12630.
26. Georgia, S. and Bhushan, A. (2004) Beta cell replication is the primary mechanism for maintaining postnatal beta cell mass. *J. Clin. Invest.*, **114**, 963–968.
27. Kushner, J.A., Ciemerych, M.A., Sicinska, E., Wartschow, L.M., Teta, M., Long, S.Y., Sicinski, P. and White, M.F. (2005) Cyclins D2 and D1 are essential for postnatal pancreatic beta-cell growth. *Mol. Cell. Biol.*, **25**, 3752–3762.
28. Barone, M.V., Crozat, A., Tabaee, A., Philipson, L. and Ron, D. (1994) CHOP (GADD153) and its oncogenic variant, TLS-CHOP, have opposing effects on the induction of G1/S arrest. *Genes Dev.*, **8**, 453–464.
29. Kim, D.-G., You, K.-R., Liu, M.-J., Choi, Y.-K. and Won, Y.-S. (2002) GADD153-mediated anticancer effects of *N*-(4-hydroxyphenyl)retinamide on human hepatoma cells. *J. Biol. Chem.*, **277**, 38930–38938.
30. Marciniak, S.J., Yun, C.Y., Oyadomari, S., Novoa, I., Zhang, Y., Jungreis, R., Nagata, K., Harding, H.P. and Ron, D. (2004) CHOP induces death by promoting protein synthesis and oxidation in the stressed endoplasmic reticulum. *Genes Dev.*, **18**, 3066–3077.
31. Hollander, M.C., Poola-Kella, S. and Fornace, A.J., Jr (2003) Gadd34 functional domains involved in growth suppression and apoptosis. *Oncogene*, **22**, 3827–3832.
32. Yagi, A., Hasegawa, Y., Xiao, H., Haneda, M., Kojima, E., Nishikimi, A., Hasegawa, T., Shimokata, K. and Isobe, K. (2003) GADD34 induces p53 phosphorylation and p21/WAF1 transcription. *J. Cell. Biochem.*, **90**, 1242–1249.
33. McBain, S.C. and Morgan, N.G. (2003) Functional effects of expression of wolframin-antisense transcripts in BRIN-BD11 beta-cells. *Biochem. Biophys. Res. Commun.*, **307**, 684–688.
34. Sherr, C.J. and Roberts, J.M. (1999) CDK inhibitors: positive and negative regulators of G1-phase progression. *Genes Dev.*, **13**, 1501–1512.
35. Cozar-Castellano, I., Weinstock, M., Haughty, M., Velazquez-Garcia, S., Sipula, D. and Stewart, A.F. (2006) Evaluation of β-cell replication in mice transgenic for hepatocyte growth factor and placental lactogen. Comprehensive characterization of the G1/S regulatory proteins reveals unique involvement of $p21^{CIP1}$. *Diabetes*, **55**, 70–77.
36. Yang, L., Sara, G., Carlson, S.G., McBurney, D. and Horton, W.E., Jr (2005) Multiple signals induce endoplasmic reticulum stress in both primary and immortalized chondrocytes resulting in loss of differentiation, impaired cell growth, and apoptosis. *J. Biol. Chem.*, **280**, 31156–31165.
37. Zu, K., Bihani, T., Lin, A., Park, Y.M., Mori, K. and Ip, C. (2006) Enhanced selenium effect on growth arrest by BiP/GRP78 knockdown in p53-null human prostate cancer cells. *Oncogene*, **25**, 546–554.
38. Uchida, T., Nakamura, T., Hashimoto, N., Matsuda, T., Kotani, K., Sakaue, H., Kido, Y., Hayashi, Y., Nakayama, K.I., White, M.F. and Kasuga, M. (2005) Deletion of Cdkn1b ameliorates hyperglycemia by maintaining compensatory hyperinsulinemia in diabetic mice. *Nat. Med.*, **11**, 175–182.
39. Shi, Y., Taylor, S.I., Tan, S.L. and Sonenberg, N. (2003) When translation meets metabolism: multiple links to diabetes. *Endocr. Rev.*, **24**, 91–101.
40. Yoshida, H., Haze, K., Yanagi, H., Yura, T. and Mori, K. (1998) Identification of the *cis*-acting endoplasmic reticulum stress response element responsible for transcriptional induction of mammalian glucose-regulated proteins. *J. Biol. Chem.*, **273**, 33741–33749.
41. Lee, A.S. (2005) The ER chaperone and signaling regulator GRP78/Bip as a monitor of endoplasmic reticulum stress. *Methods*, **35**, 373–381.
42. Niwa, H., Yamamura, K. and Miyazaki, J. (1991) Efficient selection for high-expression transfectants with a novel eukaryotic vector. *Gene*, **108**, 193–199.
43. Tashiro, F., Niwa, H. and Miyazaki, J. (1999) Constructing adenoviral vectors by using the circular form of the adenoviral genome cloned in a cosmid and the Cre-loxP recombination system. *Hum. Gene Ther.*, **10**, 1845–1852.

Am J Physiol Endocrinol Metab 290: E308–E316, 2006.
First published September 27, 2005; doi:10.1152/ajpendo.00131.2005.

Cell type-specific activation of metabolism reveals that β-cell secretion suppresses glucagon release from α-cells in rat pancreatic islets

Rui Takahashi,[1] Hisamitsu Ishihara,[1] Akira Tamura,[1] Suguru Yamaguchi,[1] Takahiro Yamada,[1] Daisuke Takei,[1] Hideki Katagiri,[2] Hitoshi Endou,[3] and Yoshitomo Oka[1]

Divisions of [1]Molecular Metabolism and Diabetes and [2]Advanced Therapeutics for Metabolic Diseases, Tohoku University Graduate School of Medicine, Sendai, Miyagi; and [3]Department of Pharmacology and Toxicology, Kyorin University School of Medicine, Mitaka, Tokyo, Japan

Submitted 22 March 2005; accepted in final form 19 September 2005

Takahashi, Rui, Hisamitsu Ishihara, Akira Tamura, Suguru Yamaguchi, Takahiro Yamada, Daisuke Takei, Hideki Katagiri, Hitoshi Endou, and Yoshitomo Oka. Cell type-specific activation of metabolism reveals that β-cell secretion suppresses glucagon release from α-cells in rat pancreatic islets. *Am J Physiol Endocrinol Metab* 290: E308–E316, 2006. First published September 27, 2005; doi:10.1152/ajpendo.00131.2005.—Abnormal glucagon secretion is often associated with diabetes mellitus. However, the mechanisms by which nutrients modulate glucagon secretion remain poorly understood. Paracrine modulation by β- or δ-cells is among the postulated mechanisms. Herein we present further evidence of the paracrine mechanism. First, to activate cellular metabolism and thus hormone secretion in response to specific secretagogues, we engineered insulinoma INS-1E cells using an adenovirus-mediated expression system. Expression of the Na^+-dependent dicarboxylate transporter (NaDC)-1 resulted in 2.5- to 4.6-fold ($P < 0.01$) increases in insulin secretion in response to various tricarboxylic acid cycle intermediates. Similarly, expression of glycerol kinase (GlyK) increased insulin secretion 3.8- or 4.2-fold ($P < 0.01$) in response to glycerol or dihydroxyacetone, respectively. This cell engineering method was then modified, using the Cre-*loxP* switching system, to activate β-cells and non-β-cells separately in rat islets. NaDC-1 expression only in non-β-cells, among which α-cells are predominant, caused an increase (by 1.8-fold, $P < 0.05$) in glucagon secretion in response to malate or succinate. However, the increase in glucagon release was prevented when NaDC-1 was expressed in whole islets, i.e., both β-cells and non-β-cells. Similarly, an increase in glucagon release with glycerol was observed when GlyK was expressed only in non-β-cells but not when it was expressed in whole islets. Furthermore, dicarboxylates suppressed basal glucagon secretion by 30% ($P < 0.05$) when NaDC-1 was expressed only in β-cells. These data demonstrate that glucagon secretion from rat α-cells depends on β-cell activation and provide insights into the coordinated mechanisms underlying hormone secretion from pancreatic islets.

pancreatic islet; paracrine regulation; glucagon secretion; cell activation

PANCREATIC ISLETS OF LANGERHANS play a central role in glucose homeostasis. In diabetic patients, not only insulin but also glucagon secretion is impaired. Basal levels of serum glucagon are elevated, and a rise in blood glucose fails to inhibit, and can paradoxically even stimulate, glucagon release in subjects with diabetes (14). In addition, the glucagon secretory response is impaired when circulating glucose drops (11), which may result in life-threatening hypoglycemia in patients treated with insulin. This unresponsiveness to hypoglycemia makes precise glycemic management difficult (8), although strict control is known to be essential for preventing diabetic complications (38). Therefore, it is important to understand the mechanisms whereby glucagon secretion is regulated by nutrients.

Three types of regulatory mechanisms have been proposed by which nutrients, such as glucose, suppress glucagon secretion. The first is a direct action of glucose on α-cells (16, 23). Glucose metabolism in α-cells is considered to generate signals that inhibit glucagon secretion, whereas glucose metabolism increases insulin secretion in β-cells. Therefore, intracellular signaling arising from glucose metabolism might differ between the two cell types, although α-cells also express molecules essential for stimulus-secretion coupling in β-cells, including ATP-sensitive K^+ (K_{ATP}) channels (3, 5). The second mechanism involves modulation by neighboring endocrine cells, such as β- (2, 10, 13, 17, 33, 39) and δ-cells (7, 34). Several molecules, including insulin (2, 13, 33), Zn^{2+} (10, 17), γ-aminobutyric acid (GABA; see Ref. 39), and somatostatin (7, 34), have been postulated to be mediators of these inhibitory effects. Autonomic regulation is the third mechanism (6, 37) and might be clinically important for responses to hypoglycemia, although in humans the glucagon response to hypoglycemia from a transplanted (denerved) pancreas is intact, arguing against this possibility (9).

Studies of stimulus-secretion coupling in β-cells, the predominant cell type of islets, have made great progress in recent decades (20). In contrast, α-cell research has been hampered because of difficulties in getting sufficient numbers of this cell type. Nonetheless, an earlier study has found important characteristics of α-cells (32), and several recent studies have discovered interesting features of this cell type. Characterization of electrical activity and calcium dynamics revealed a unique ion channel composition in α-cells (12). In addition, pyruvate induces glucagon secretion from α-cells (17) but does not stimulate insulin secretion from β-cells. This is probably because α-cells have a transporting system for pyruvate but β-cells do not. This observation suggests that metabolized nutrients can induce exocytosis in α-cells as is the case in β-cells. However, when the pancreas is perfused or islets are stimulated with metabolized nutrients such as glucose, insulin secretion is stimulated, whereas glucagon secretion is suppressed.

Address for reprint requests and other correspondence: H. Ishihara, Div. of Molecular Metabolism and Diabetes, Tohoku Univ. Graduate School of Medicine, 2–1 Seiryo-machi, Aoba-ku, Sendai, Miyagi 980-8575, Japan (e-mail: ishihara-tky@umin.ac.jp).

The costs of publication of this article were defrayed in part by the payment of page charges. The article must therefore be hereby marked "*advertisement*" in accordance with 18 U.S.C. Section 1734 solely to indicate this fact.

In this study, to gain insight into the regulatory mechanism governing glucagon secretion in islets, we have established a method to activate cellular metabolism in β-cells and non-β-cells separately. For this purpose, we have expressed Na^+-dependent dicarboxylate transporter (NaDC)-1 or glycerol kinase (GlyK) in β-cells and/or non-β-cells. Using this method, we showed rat α-cells to secret glucagon when metabolically activated in the absence of β-cell activation. In addition, basal glucagon secretion was shown for the first time to be suppressed by β-cell activation. These data contribute to our understanding of the regulation of islet hormone secretion, providing insights that are anticipated to be of value in managing hypoglycemia and hyperglycemia in subjects with diabetes.

MATERIALS AND METHODS

Generation of recombinant adenoviruses bearing rat GlyK cDNA (AdRIPHAGlyK and AdCAGlxHAGlyKlx) and NaDC-1 cDNA (AdRIPNaDC and AdCAGlxNaDClx). Rat GlyK cDNA (31) was amplified using rat liver total RNA. An entire coding region was sequenced and subcloned downstream of the hemagglutinin (HA)-epitope sequence. Rat NaDC-1 cDNA was as described previously (36). A *Sph*I-*Spe*I fragment of HA-tagged GlyK (HAGlyK) cDNA and a *Sal*I-*Sma*I fragment of NaDC-1 cDNA were ligated between the 410-bp fragment of the rat insulin 1 promoter and the rabbit β-globin poly(A) signal region. The resulting expression units were used for generation of AdRIPHAGlyK and AdRIPNaDC by the methods described previously (27). Rat GlyK and NaDC-1 cDNA were also subcloned between two *lox*P sequences and ligated under the CAG (a transcriptional unit composed of the cytomegalovirus enhancer, the actin promoter, and the globin intron) promoter unit (28). Recombinant viruses harboring these expression units were then generated (AdCAGlxHAGlyKlx and AdCAGlxNaDClx). AdCAGlacZ (27) expressing β-galactosidase was used as a control adenovirus. AdRIPNCre was renamed from AdInsPNCre generated as described previously (17). Adenovirus titers were measured by the method described previously (27).

Isolation of rat islets and infection with recombinant adenoviruses. Rat islets were prepared by retrograde collagenase infusion through the common bile duct and hand picked under the microscope. Isolated islets were infected with the recombinant adenoviruses at 1.2×10^6 plaque-forming units (PFU)/islet in 1.0 ml medium for 60 min. In the case of combined infection of AdCAGlxNaDClx plus AdRIPNCre or AdCAGlxHAGlyKlx plus AdRIPNCre, the amount of AdRIPNCre was four times greater than the others, with a total amount of 1.2×10^6 PFU/islet.

Immunoblot analysis. INS-1E cells (25) were infected with either AdRIPHAGlyK or AdRIPNaDC at multiplicity of infection (MOI) of 100, cultured for 2 days, and directly dissolved in the SDS sample buffer. Proteins were subjected to SDS-PAGE and were transferred to nitrocellulose membranes. Membranes were probed with rabbit anti-rat NaDC-1 antibody raised against the carboxy-terminal peptide (1:500; see Ref. 36) or with anti-HA tag antibody (1:200; Santa Cruz Biotechnology, Santa Cruz, CA) for 1 h at room temperature and then incubated for 1 h with anti-rabbit IgG (1:1,000) conjugated with horseradish peroxidase, respectively. Detection was accomplished with chemiluminescence (ECL; Amersham Biosciences, Piscataway, NJ).

Immunocytochemical analyses. INS-1E cells infected with either AdRIPHAGlyK or AdRIPNaDC at an MOI of 100 were incubated with anti-rat NaDC-1 antibody (1:500) or with anti-HA tag antibody (1:200) for 1 h at room temperature and then incubated for 1 h with FITC-conjugated anti-rabbit IgG (1:500; Jackson ImmunoResearch, West Grove, PA). Islets infected with AdRIPHAGlyK, AdCAGlxHAGlyKlx alone, or AdCAGlxHAGlyKlx plus AdRIPNCre were dispersed on coverslips. Cells were then fixed with 4% paraformaldehyde and incubated with anti-HA tag antibody (1:200) followed by incubation with FITC-conjugated anti-rabbit IgG. Insulin and glucagon were also stained using mouse monoclonal antibodies against these hormones (1:1,000; Sigma-Aldrich, Tokyo, Japan) and Texas red-conjugated anti-mouse IgG (1:500; Jackson ImmunoResearch).

Hormone secretion. INS-1E cells (0.2×10^6 cells/well of 24-well plates) or islets (10 islets/tube) infected with recombinant adenoviruses were incubated over a period of 60 min in 1 ml of Krebs-Ringer-bicarbonate-HEPES buffer [140 mM NaCl, 3.6 mM KCl, 0.5 mM NaH_2PO_4, 0.5 mM $MgSO_4$, 1.5 mM $CaCl_2$, 2 mM $NaHCO_3$, 10 mM HEPES (pH 7.4), and 0.1% BSA] containing 2.5 mM glucose plus indicated stimulators. Insulin and glucagon were detected by RIA kits (Linco, St. Louis, MO).

Statistical analyses. Data are presented as means ± SE. Differences between groups were assessed by Student's *t-test* for unpaired data.

RESULTS

Expression of NaDC-1 resulted in cell activation in response to dicarboxylates. We first sought to establish a means of activating metabolism in specific cell types of pancreatic islets to study *1*) the roles of α-cell nutrient metabolism in glucagon secretion and *2*) whether activation of neighboring β-cells in response to nutrient metabolism modulates α-cell secretion. It was previously shown that β-cells expressing monocarboxylate transporter (MCT-1) metabolize pyruvate and secrete insulin in response to the monocarboxylate (18). Similarly, insulin secretion is reportedly stimulated in β-cells expressing GlyK in response to glycerol (1, 29). These data suggested that cells normally unresponsive to some nutrients can be activated by expressing protein(s) needed for their metabolism. We tested whether tricarboxylic acid (TCA) cycle intermediates alter insulin and glucagon secretion in isolated rat islets and found α-ketoglutarate, succinate, fumarate, and malate to have no effects on hormone secretion in wild-type islets (Fig. 1). A membrane-permeable analog of succinate, methylsuccinate, is known to stimulate insulin secretion (24), suggesting that inability of TCA cycle intermediates to activate β-cells is attributable to low or no expression of membrane transporters for these compounds. Therefore, to activate cells, a recombinant adenovirus harboring cDNA encoding rat NaDC-1 under the rat insulin promoter (AdRIPNaDC) was constructed, with the aim of activating the cells with TCA cycle intermediates.

We first employed rat insulinoma INS-1E cells to study whether the recombinant adenovirus induces functional expression of NaDC-1, leading to increased cellular metabolism and thereby promoting insulin secretion. Western blotting using an antibody against NaDC-1 showed strong expression of NaDC-1, with the expected protein size, in insulinoma INS-1E cells infected with AdRIPNaDC (Fig. 2*A*). Immunocytochemical analysis revealed strong staining at the cell surface, although weak staining was observed inside the cell, suggesting improper targeting of some expressed membrane proteins because of forced expression (Fig. 2*B*). As shown in Fig. 2*C*, adenovirus-mediated expression of NaDC-1 made INS-1E cells responsive to various TCA cycle intermediates. Citrate, one of the tricarboxylates, existing partly in a divalent form at pH 7.4 (36), could be transported into INS-1E cells expressing NaDC-1, and thereby induced insulin secretion. A nonmetabolizable dicarboxylate, glutarate, failed to induce insulin secretion from INS-1E cells expressing NaDC-1, indi-

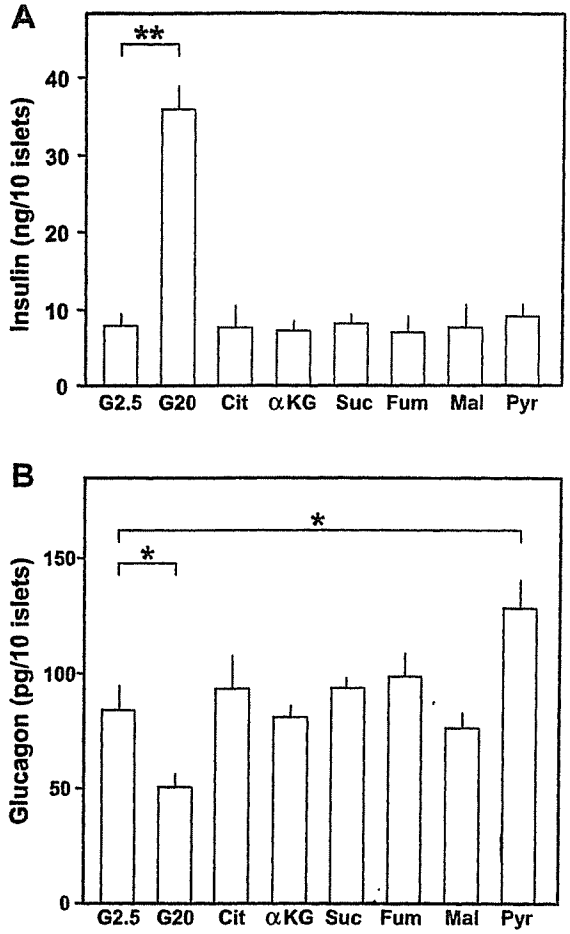

Fig. 1. Tricarboxylic acid (TCA) cycle intermediates had no effects on either insulin or glucagon secretion. Isolated islets were cultured overnight and challenged with glucose (20 mM), pyruvate (10 mM), and various TCA cycle intermediates (10 mM). Insulin (*A*) and glucagon (*B*) secreted during a 60-min incubation were measured. G2.5, 2.5 mM glucose; G20, 20 mM glucose; Cit, citrate; αKG, α-ketoglutarate; Suc, succinate; Fum, fumarate; Mal, malate; Pyr, pyruvate. Data are means ± SE; $n = 3$~7. *$P < 0.05$ and **$P < 0.01$.

cating insulin secretion evoked by dicarboxylates to be the result of activation of metabolism. In addition, insulin secretion evoked by malate was abolished by 2 mM NaN_3, a metabolic inhibitor (data not shown), further supporting this notion.

Expression of GlyK resulted in cell activation in response to glycerol. We also expressed rat GlyK to activate the cellular glycolytic pathway. Glycerol and dihydroxyacetone can enter the glycolytic pathway after GlyK-mediated conversion to glycerol 3-phosphate and dihydroxyacetone phosphate, respectively. Adenovirus-mediated introduction of HAGlyK cDNA resulted in expression of this protein in the INS-1E cell cytosol (Fig. 2, *D* and *E*). Expressed HAGlyK was functional, since INS-1E cells expressing HAGlyK secreted insulin in response to glycerol or dihydroxyacetone (Fig. 2*F*), as was reported in INS-1E cells expressing *Escherichia coli* GlyK (1, 29).

Taken together, these data indicate NaDC-1 and GlyK expressions to be effective in activating cellular metabolism in response to certain nutrients.

Cell type-specific expressions of genes in isolated islets. To study the stimulus-secretion coupling in α-cells and possible cross-talk with other pancreatic endocrine cells, we next sought to express the genes of interest in α- and β-cells separately. As was reported previously (17), the rat insulin 1 promoter has high transcription activity and specificity for β-cell-restricted expression of foreign genes. Therefore, β-cell-specific expression of NaDC-1 or HAGlyK was achieved using recombinant adenovirus vectors with the rat insulin 1 promoter (Fig. 3*A*). When islets were infected with AdRIPHAGlyK, >60% of insulin-positive cells were stained with HA (Fig. 3*D*), but none of the glucagon-positive cells expressed HAGlyK (Fig. 3*E*).

In contrast to the insulin 1 promoter for β-cells, the glucagon promoter (1.6 kbp) did not have high transcriptional activities specific for α-cells when placed in the adenoviral genome (data not shown). To increase expression in α-cells, a dual-adenovirus approach was previously developed (17); one adenovirus produces Cre recombinase under the glucagon promoter, and the other virus expresses the desired genes under the potent CAG promoter unit (28) once the intervening sequence is excised by Cre recombinase (17). Although the strategy increased the expression levels of reporter genes, such as luciferase, in α-cells, it did not significantly increase the activities of cellular enzymes or transporters, such as glucokinase and MCT-1 (data not shown). We then raised the recombinant virus titer. However, a high titer of virus with the glucagon promoter also induced expression in cells other than α-cells (data not shown). We therefore did not employ the glucagon promoter in this study but rather devised a method employing the insulin 1 promoter and the Cre-*loxP* system.

As shown in Fig. 3*C*, a cDNA floxed with *loxP* sequences was placed downstream from the CAG promoter unit (28) that enables transcription in any cell type. This expression unit was then introduced into islet cells, together with the insulin promoter-Cre adenovirus (AdRIPNCre; see Ref. 17). The cDNA was expected to be removed from the unit by the Cre recombinase in the β-cell, allowing expression of the genes of interest in non-β-cells, a cell population where α-cells are predominant. Indeed, when rat islets were infected with AdCAGlxHAGlyKlx and AdRIPNCre, ~70% of glucagon-positive cells was stained with HA (Fig. 3, *H* and *I*). More than 80% of HA-positive cells were observed to be stained with glucagon, and <10% were insulin positive, although HA staining was occasionally observed in somatostatin-positive cells and fibroblast-like cells (data not shown). When islets were infected with AdCAGlxHAGlyKlx alone (Fig. 3*B*), ~60% of β-cells (Fig. 3*F*) and 65% of α-cells (Fig. 3*G*) expressed HAGlyK.

α-Cell activation triggered glucagon secretion when β-cells remained nonactivated. To study the role of nutrient metabolism in glucagon secretion from α-cells, isolated rat islets were infected with AdCAGlxNaDClx plus AdRIPNCre and challenged with succinate or malate. As shown in Fig. 4, *A* and *B*, glucagon secretion was increased by 80%, without changes in insulin secretion. These effects were abolished by 2 mM NaN_3, indicating the observed glucagon secretion to be due to activation of cellular metabolism of the dicarboxylates. When islets were infected with AdCAGlxHAGlyKlx plus AdRIPNCre and then challenged with 10 mM glycerol, insulin secretion did not change (Fig. 4*C*) and glucagon secretion tended to increase, but the differences did not reach statistical significance (Fig. 4*D*).

In contrast, when α-cells were activated together with β-cells by infecting islets with AdCAGlxNaDClx alone, i.e., without AdRIPNCre (Fig. 5, *A* and *B*), insulin secretion was increased by more than threefold in response to 10 mM malate

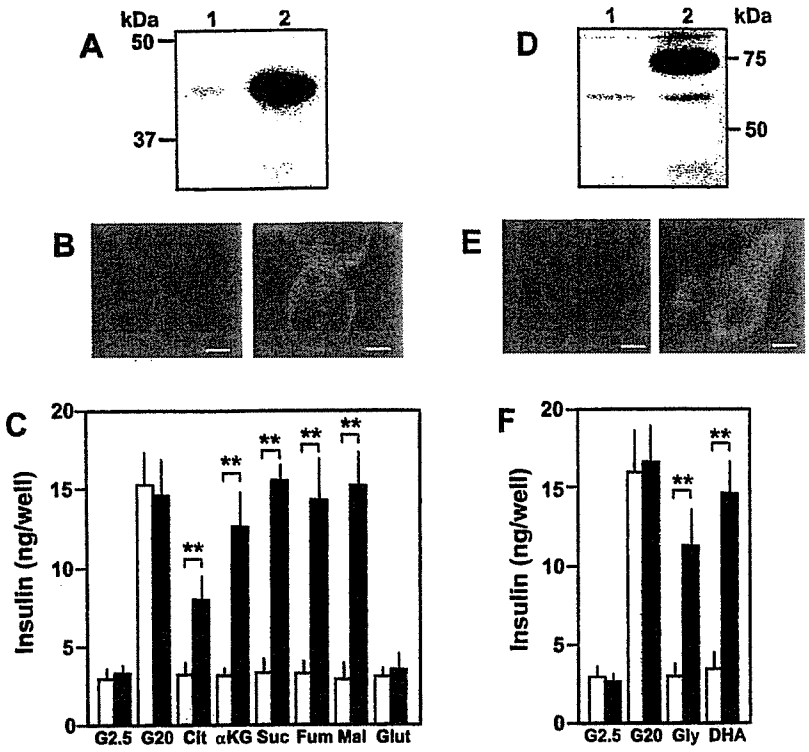

Fig. 2. Adenovirus-mediated Na^+-dependent dicarboxylate transporter (NaDC)-1 or glycerol kinase (GlyK) expression in INS-1E cells. *A*: INS-1E cells infected with either AdCAGlacZ (*lane 1*) or AdRIPNaDC (*lane 2*) were subjected to SDS-PAGE and probed with an anti-NaDC-1 antibody. *B*: INS-1E cells infected with either AdCAGlacZ (*left*) or AdRIPNaDC (*right*) were stained with anti-NaDC-1 antibody. Bars, 4 μm. *C*: INS-1E cells infected with either AdCAGlacZ (open bars) or AdRIPNaDC (filled bars) were challenged with 20 mM glucose or various TCA cycle intermediates (10 mM). Insulin secreted during a 60-min incubation was measured. Data are means ± SE; $n = 5$. $^{**}P < 0.01$. Glut, glutarate. *D*: INS-1E cells infected with either AdCAGlacZ (*lane 1*) or AdRIPHAGlyK (*lane 2*) were subjected to SDS-PAGE and probed with an anti-hemagglutinin (HA) antibody. *E*: INS-1E cells infected with either AdCAGlacZ (*left*) or AdRIPHAGlyK (*right*) were stained with an anti-HA antibody. Bars, 4 μm. *F*: INS-1E cells infected with either AdCAGlacZ (open bars) or AdRIPHAGlyK (filled bars) were challenged with 20 mM glucose, 10 mM glycerol (Gly), or 10 mM dihydroxyacetone (DHA). Insulin secreted during a 60-min incubation was measured. Data are means ± SE; $n = 4$. $^{**}P < 0.01$.

or succinate, whereas glucagon release was unchanged. Similarly, AdCAGlxHAGlyKlx infection increased insulin (by 2.5-fold) but not glucagon secretion with a 10 mM glycerol challenge (Fig. 5, *C* and *D*). These data indicate that α-cell activation dose not lead to glucagon secretion when β-cells are activated simultaneously.

Recent studies have postulated several molecules, including insulin (2, 13, 33), Zn^{2+} (10, 17), and GABA (39), as mediators of β-cell inhibitory effects on glucagon secretion. During succinate stimulation, insulin secreted from β-cells expressing NaDC-1 amounted to ~25 ng/ml (Fig. 5*A*). We therefore examined whether this amount of insulin inhibits glucagon secretion from islets expressing NaDC-1 in α- but not β-cells. As shown in Fig. 6, succinate-stimulated glucagon secretion from islets infected with AdCAGlxNaDClx plus AdRIPNCre was significantly suppressed by 25 ng/ml insulin, indicating that insulin mediates inhibitory effects of β-cells on glucagon secretion. However, the suppression seemed incomplete, sug-

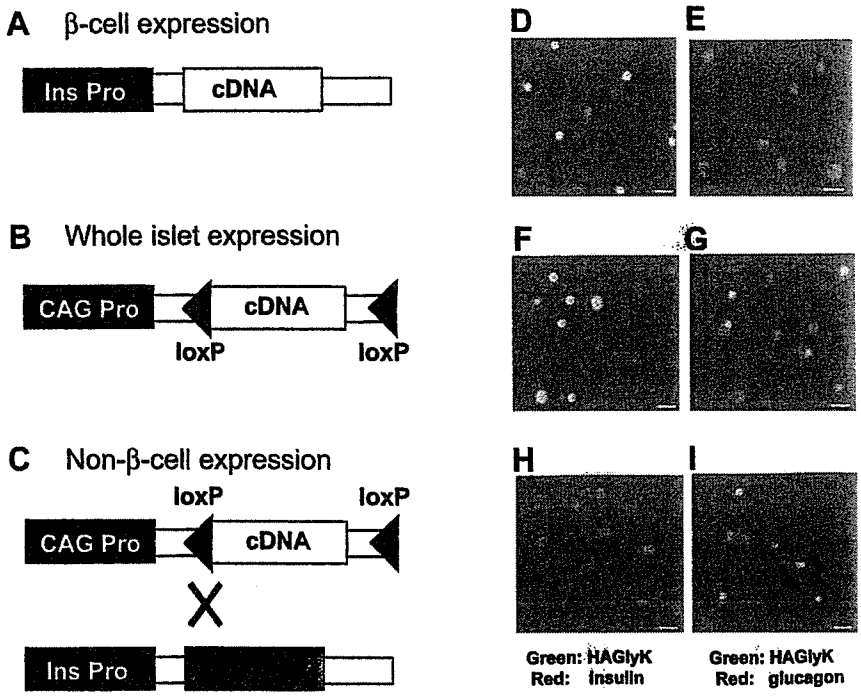

Fig. 3. Selective gene expression method for β- and non-β-cells in islets. *A–C*: schematic representation of adenoviruses for expression in β-cells (*A*), whole islet cells (*B*), and non-β-cells (*C*). NCre, nuclear targeted Cre recombinase; CAG, a transcriptional unit composed of the cytomegalovirus enhancer, the actin promoter, and the globin intron (28). *D* and *E*: islets infected with AdRIPHAGlyK were dispersed and stained with an anti-HA (green) antibody (*D* and *E*) together with anti-insulin (red; *D*) or anti-glucagon (red; *E*) antibody. *F* and *G*: islets infected with AdCAGlxHAGlyKlx alone were dispersed and stained with an anti-HA (green) antibody (*F* and *G*) together with anti-insulin (red; *F*) or anti-glucagon (red; *G*) antibody. *H* and *I*: islets infected with AdCAGlx-HAGlyKlx plus AdRIPNCre were dispersed and stained with an anti-HA (green) antibody (*H* and *I*) together with anti-insulin (red; *H*) or anti-glucagon (red; *I*) antibody. Bars, 10 μm. Colocalization resulted in yellow.

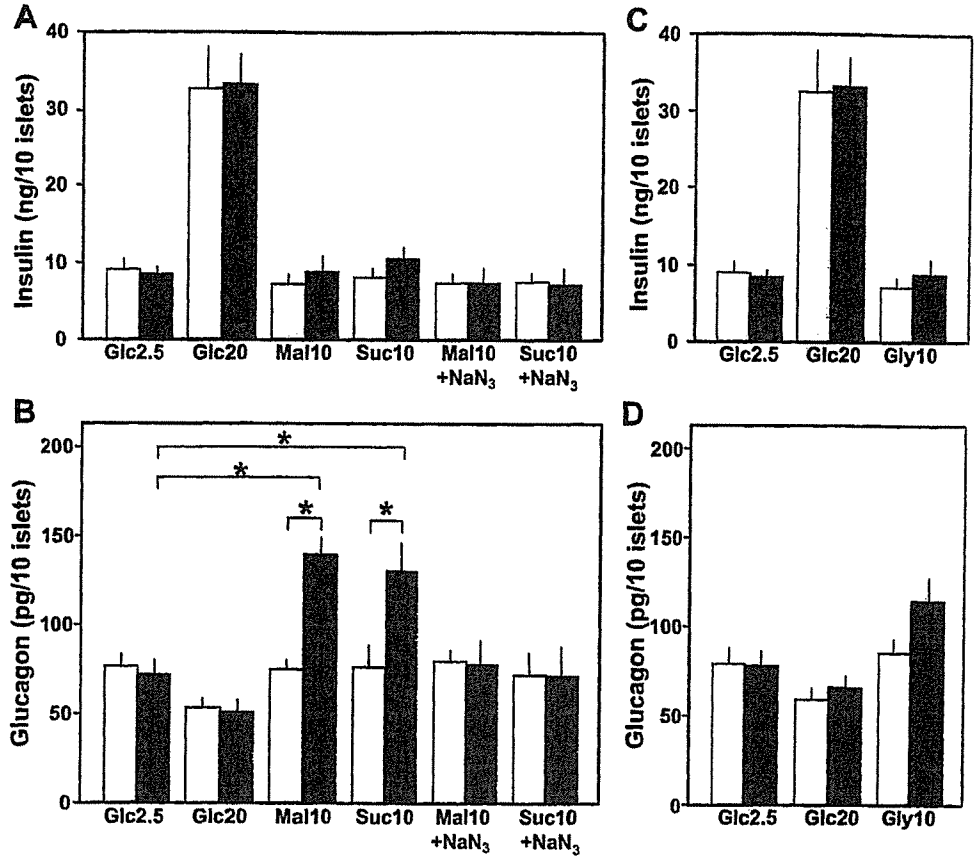

Fig. 4. Selective α-cell activation induced glucagon secretion. *A* and *B*: isolated islets (10 islets/tube) infected with AdCAGlacZ plus AdRIPNCre (open bars) or AdCAGlx-NaDClx plus AdRIPNCre (filled bars) were challenged with 20 mM glucose, 10 mM malate (Mal10), or 10 mM succinate (Suc10) with or without 2 mM NaN_3. Insulin (*A*) and glucagon (*B*) secreted during a 60-min incubation were measured; $n = 3\sim5$. $^*P < 0.05$. *C* and *D*: isolated islets (10 islets/tube) infected with AdCAGlacZ plus AdRIPNCre (open bars) or AdCAGlxHAGlyKlx plus AdRIPNCre (filled bars) were challenged with 20 mM glucose, or 10 mM glycerol (Gly10). Insulin (*C*) and glucagon (*D*) secreted during a 60-min incubation were measured; $n = 4$.

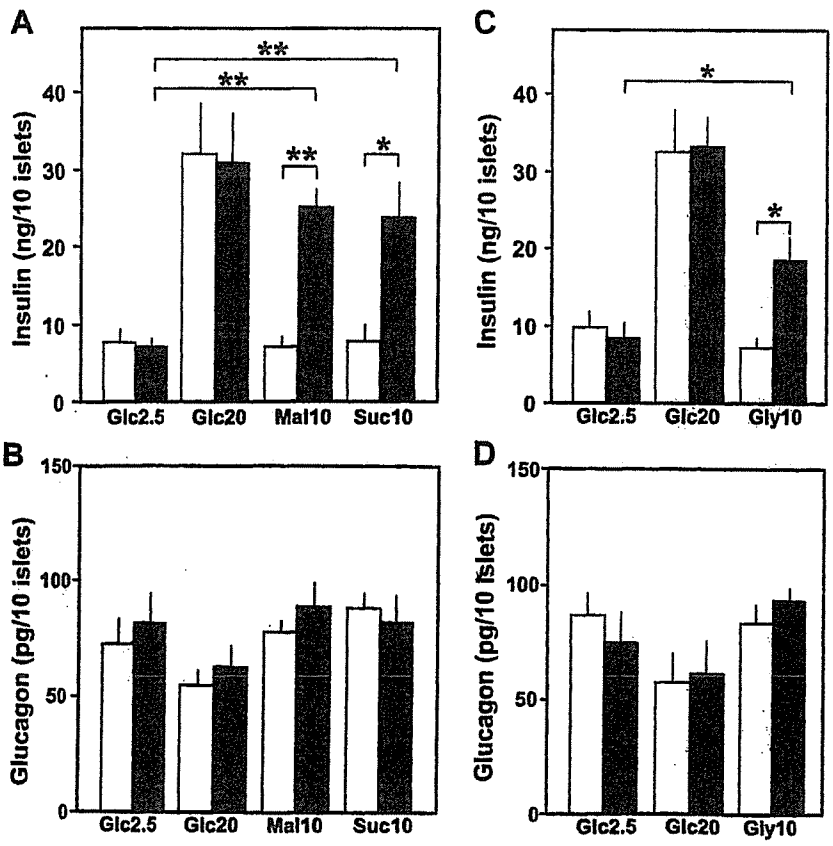

Fig. 5. Simultaneous α- and β-cell activation induced insulin but not glucagon secretion. *A* and *B*: isolated islets (10 islets/tube) infected with AdCAGlacZ (open bars) or AdCA-GlxNaDClx (filled bars) were challenged with 20 mM glucose, 10 mM malate, or 10 mM succinate. Insulin (*A*) and glucagon (*B*) secreted during a 60-min incubation were measured; $n = 4\sim6$. $^*P < 0.05$ and $^{**}P < 0.01$. *C* and *D*: isolated islets (10 islets/tube) infected with AdCAGlacZ (open bars) or AdCAGlxHAGlyKlx (filled bars) were challenged with 20 mM glucose, or 10 mM glycerol. Insulin (*C*) and glucagon (*D*) secreted during a 60-min incubation were measured; $n = 4$. $^*P < 0.05$.

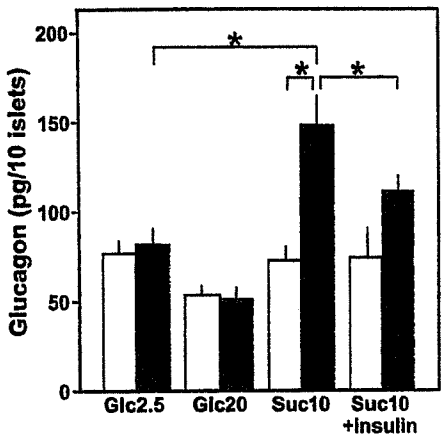

Fig. 6. Insulin suppressed succinate-stimulated glucagon secretion. Isolated islets (10 islets/tube) infected with AdCAGlacZ plus AdRIPNCre (open bars) or AdCAGlxNaDClx plus AdRIPNCre (filled bars) were challenged with 20 mM glucose, 10 mM succinate alone, or 10 mM succinate with 25 ng/ml insulin. Glucagon secreted during a 60-min incubation was measured; $n = 4$. $^*P < 0.05$.

gesting another molecule(s) is also important in suppression of glucagon secretion by β-cell activation.

β-Cell activation increased insulin secretion and decreased basal glucagon secretion. We next studied whether basal glucagon secretion was altered by β-cell activation. For this purpose, NaDC-1 was expressed only in β-cells by infecting islets with AdRIPNaDC. When these islets were challenged with 10 mM malate or succinate, insulin secretion more than doubled (Fig. 7*A*). Interestingly, glucagon secretion from the same islets was reduced significantly, by 30% (Fig. 7*B*). Similar modulation of hormone secretion was observed when islets were infected with AdRIPGlyK; insulin secretion was increased significantly, by 1.7-fold, in response to 10 mM glycerol (Fig. 7*C*), whereas glucagon secretion tended to decrease, although not to a statistically significant degree (Fig. 7*D*).

DISCUSSION

Abnormal nutrient-mediated modulation of glucagon secretion is often associated with diabetes mellitus. However, the mechanisms whereby nutrients modulate glucagon secretion remain poorly understood. Paracrine modulation by β- or δ-cells is among the postulated mechanisms. Herein we provide further evidence that glucagon secretion from α-cells is stimulated by nutrient metabolism in the absence of β-cell activation but it is suppressed when β-cells are activated.

We first demonstrated, employing NaDC-1 expression, that TCA cycle intermediates induce insulin secretion from β-cells engineered to transport these substrates. It was previously reported that pyruvate and lactate stimulate insulin secretion from β-cells expressing MCT-1 and lactate dehydrogenase (LDH) but not from normal β-cells (18). This was interpreted as low levels of MCT-1 and LDH expression protecting β-cells

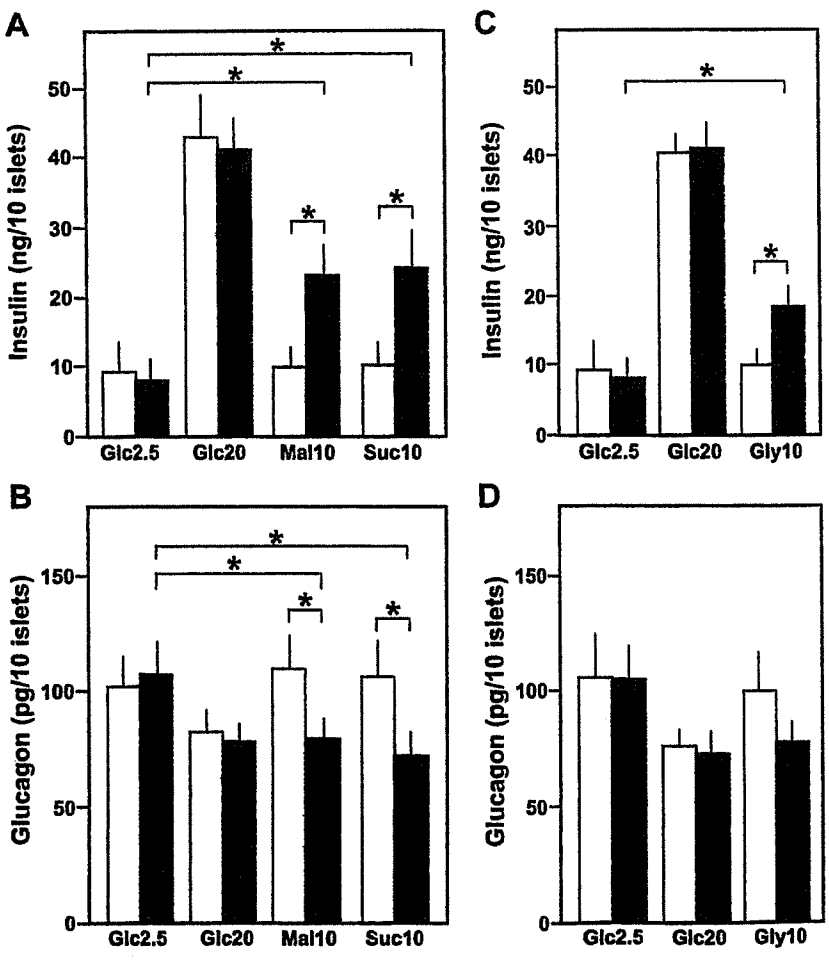

Fig. 7. Selective β-cell activation inhibited glucagon secretion. *A* and *B*: isolated islets (10 islets/tube) infected with AdCAGlacZ (open bars) or AdRIPNaDC (filled bars) were challenged with 20 mM glucose, 10 mM malate, or 10 mM succinate. Insulin (*A*) and glucagon (*B*) secreted during a 60-min incubation were measured. $^*P < 0.05$; $n = 5$. *C* and *D*: isolated islets (10 islets/tube) infected with AdCAGlacZ (open bars) or AdRIPHAGlyK (filled bars) were challenged with 20 mM glucose or 10 mM glycerol. Insulin (*C*) and glucagon (*D*) secreted during a 60-min incubation were measured. $^*P < 0.05$; $n = 4$.

from the stimulatory effects of pyruvate and lactate, which could otherwise cause undesired insulin secretion in catabolic states, such as during exercise. Similarly, the present data suggest that low levels of NaDC-1 expression protect β-cells from the stimulatory effects of dicarboxylates and confer glucose selectivity on insulin secretion.

A major part of the present study was based on the method we devised to activate cellular metabolism in β-cells and non-β-cells, separately, in primary rat islets by specifically expressing NaDC-1 or GlyK in β-cells and non-β-cells. Employing this innovative approach, we showed TCA cycle intermediates, succinate and malate, to induce glucagon secretion when NaDC-1 is expressed in α-cells. Stimulation of glucagon secretion was previously demonstrated in intact islets challenged with another mitochondrial substrate, pyruvate, which exerts essentially no stimulatory effects on β-cells (17). In subjects with type 1 diabetes, glucose reportedly failed to suppress, or even slightly stimulated, glucagon secretion (14). Abnormal glucagon secretion in response to glucose was also reported in islets from insulin-deficient Chinese hamsters (19). The present data, obtained employing NaDC-1 expression, thus support the concept of α-cells having an inherent capacity to increase glucagon secretion in response to nutrients under certain circumstances, i.e., in the absence of β-cell effects. GlyK expression in α-cells tended to increase glucagon secretion in response to glycerol, but not to a statistically significant degree (Fig. 3*D*). This might be because the coupling of glycolysis and mitochondrial metabolism is less efficient in α-cells than in β-cells, as previously suggested (35). In contrast, dicarboxylates directly stimulate mitochondrial metabolism in cells expressing NaDC-1, thereby possibly producing a significant increase in glucagon secretion.

The concept of α-cells having an inherent capacity to increase glucagon secretion in response to nutrients has been reinforced recently by the demonstration of glucagon secretion stimulated by glucose from purified rat α-cells (10). An earlier study (32), however, reported that glucose inhibited glucagon secretion induced by an amino acid mixture in purified α-cells. Thus direct action on α-cells could be multiple, both inhibitory and stimulatory in nature. Glucose reportedly promotes the filling of the endoplasmic reticulum Ca^{2+} stores in α-cells (23) as in β-cells (20). In the presence of an amino acid mixture, glucose inhibitory effects could attenuate the rise in cytosolic Ca^{2+} induced by amino acids, whereas glucose stimulatory effects could be masked by amino acid-stimulated Ca^{2+} elevation.

Glucagon secretion stimulated by pyruvate was previously shown to be suppressed by activation of β-cells expressing MCT-1 (17). Similar inhibition of activated glucagon secretion by β-cell secretory activities was recently reported in β-cell-specific Foxa2 knockout mice (22). Islets from these mice secreted insulin in response to an amino acid mixture, and, interestingly, the glucagon secretion that is normally seen in the wild-type islets in response to amino acids was abolished in the mutant islets. This result is consistent with the notion that suppression of activated glucagon secretion is attributable to β-cell secretory activities. In the present study, for the first time, we have shown basal glucagon secretion to also be suppressed by β-cell activation. In addition, in NaDC-1-expressing cells, glucose stimulated insulin secretion more potently (an ~4.5-fold increase) than dicarboxylates (an ~2-fold increase; Fig. 7*A*), whereas glucose and dicarboxylates suppressed glucagon secretion to a similar extent (~30%). We speculated that this is because, when islets were challenged with glucose, α-cells were also activated for glucagon secretion, which counteracted the suppressing effect exerted by β-cell secretory activities. Recent studies demonstrated that insulin (2, 13, 33), Zn^{2+} (10, 17), and GABA (39) are candidates for β-cell-derived inhibitory substances of glucagon secretion in rat islets. Our observation of inhibitory effects of insulin on succinate-stimulated glucagon secretion from islets expressing NaDC-1 in α- but not β-cells supports this notion about the role of insulin. To study roles of Zn^{2+} and GABA, it is crucial to determine amounts of these molecules secreted from β-cells during nutrient stimulation. Further studies are needed to elucidate the molecular basis of β-cell inhibitory effects.

Glucagon secretion was reported to depend differentially on Ca^{2+} influx through N- and L-type Ca^{2+} channels (12, 16). N-type Ca^{2+} channels operate predominantly under basal conditions and L-type Ca^{2+} channels in the stimulated state. β-Cell activation suppressed glucagon secretion regardless of whether α-cells were in the basal (Fig. 7*B*) or the stimulated state (Fig. 4*B*; see Refs. 17 and 22), suggesting the suppressed glucagon secretion to possibly be due to direct inhibition of two Ca^{2+} channels or to indirect inhibition of Ca^{2+} channels resulting from prevention of membrane depolarization. The latter could be achieved by opening of $GABA_A$ receptor Cl^- channels in the α-cell (39). In addition, prevention of membrane depolarization is also brought about by activation of K_{ATP} channels, which is reportedly induced by the β-cell secretory products, Zn^{2+} (4, 10) and insulin (10, 21). However, involvement of K_{ATP} channels in regulating glucagon secretion is controversial, since different glucagon responses were demonstrated in the following two mutant islets lacking functional K_{ATP} channels: preserved glucagon responses from islets deficient in one of the K_{ATP} channel subunits, Kir6.2 (26), and no response from islets deficient in another subunit, sulfonylurea receptor 1 (16).

Although inhibition of glucagon secretion by activation of β-cells expressing NaDC-1 supports the paracrine mechanism, it does not exclude a direct inhibitory effect of glucose metabolism on glucagon secretion, especially at relatively low glucose concentrations and in the presence of stimulators of glucagon secretion, such as an amino acid mixture (see above). Two different mechanisms by which glucose directly suppresses glucagon secretion have been proposed. One involves a store-operated current, which controls a depolarizing cascade leading to opening of L-type Ca^{2+} channels in α-cells (23). Thus glucose-induced ATP generation stimulates Ca^{2+} sequestration in endoplasmic reticulum and modulates a store-operated current. Another is based on low K_{ATP} channel activity and the special ion channel composition of the α-cell (5, 15); K_{ATP} channel closure by ATP produced during glucose metabolism causes modest depolarization, which inactivates, instead of activating, voltage-gated Na^+, T- and N-type Ca^{2+}, and A-type K^+ channels participating in action potential generation. Both models are based on data obtained in mouse α-cells, in which the K_{ATP} channel density is much less than

that in rat α-cells. Rat α-cells were calculated to have nearly 100-fold more K_{ATP} channels than mouse α-cells and double the number in rat β-cells (3, 5). K_{ATP} channels couple nutrient metabolism to membrane depolarization. Therefore, in rat α-cells with a greater number of K_{ATP} channels, nutrient metabolism could induce greater changes in membrane potential compared with those in mouse α-cells, thereby allowing glucagon secretion. Thus the importance of paracrine inhibition might be species dependent. It is essential to establish the level of K_{ATP} channel expression in human α-cells and whether this channel contributes to the regulation of glucagon secretion in humans. In this context, it is noteworthy that K_{ATP} channel-blocking agents stimulated glucagon secretion in subjects with insulin-deficient type 1 diabetes (30).

In summary, our findings provide further evidence supporting the concept that α-cell exocytosis can be modulated by β-cells via a paracrine mechanism. Future studies should focus on detailed molecular analyses of stimulus-secretion coupling in α-cells under paracrine regulation. This is a promising approach to identifying new drug targets for treating α-cell abnormalities in diabetic patients.

ACKNOWLEDGMENTS

We are grateful to Y. Nagura for expert assistance.

GRANTS

This work was supported by a grant from Suzuken Memorial Foundation to H. Ishihara and a Grant-in-Aid for Scientific Research (15659213) from the Ministry of Education, Science, Sports, and Culture of Japan and a Grant-in-Aid for Research on Human Genome, Tissue Engineering (H17-genome-003) from the Ministry of Health, Labor and Welfare to Y. Oka.

REFERENCES

1. **Antinozzi PA, Ishihara H, Newgard CB, and Wollheim CB.** Mitochondrial metabolism sets the maximal limit of fuel-stimulated insulin secretion in a model pancreatic β-cell: a survey of four fuel secretagogues. *J Biol Chem* 277: 11746–11755, 2002.
2. **Banarer S, McGregor VP, and Cryer PE.** Intraislet hyperinsulinemia prevents the glucagon response to hypoglycemia despite an intact autonomic response. *Diabetes* 51: 958–965, 2002.
3. **Barg S, Galvanovskis J, Gopel SO, Rorsman P, and Eliasson L.** Tight coupling between electrical activity and exocytosis in mouse glucagon-secreting α-cells. *Diabetes* 49: 1500–1510, 2000.
4. **Bloc A, Cens T, Cruz H, and Dunant Y.** Zinc-induced changes in ionic currents of clonal rat pancreatic A-cells: activation of ATP-sensitive K^+ channels. *J Physiol* 529: 723–734, 2000.
5. **Bokvist K, Olsen HL, Hoy M, Gotfredsen CF, Holmes WF, Buschard K, Rorsman P, and Gromada J.** Characterization of sulfonylurea and ATP-regulated K^+ channels in rat pancreatic A-cells. *Pflügers Arch* 438: 428–436, 1999.
6. **Burcelin R and Thorens B.** Evidence that extrapancreatic GLUT2-dependent glucose sensors control glucagon secretion. *Diabetes* 50: 1282–1289, 2001.
7. **Cejvan K, Coy DH, and Efendic S.** Intra-islet somatostatin regulates glucagon release via type 2 somatostatin receptors in rats. *Diabetes* 52: 1176–1181, 2003.
8. **Cryer PE.** Hypoglycaemia: the limiting factor in the glycaemic management of Type I and Type II diabetes. *Diabetologia* 45: 937–948, 2002.
9. **Diem P, Redmon JB, Abid M, Moran A, Sutherland DE, Halter JB, and Robertson RP.** Glucagon, catecholamine and pancreatic polypeptide secretion in type I diabetic recipients of pancreas allografts. *J Clin Invest* 86: 2008–2013, 1990.
10. **Franklin I, Gromada J, Gjinovci A, Theander S, and Wollheim CB.** β-cell secretory products activate α-cell ATP-dependent potassium channels to inhibit glucagon release. *Diabetes* 54: 1808–1815, 2005.
11. **Gerich JE, Langlois M, Noacco C, Karam JH, and Forsham PH.** Lack of glucagon response to hypoglycemia in diabetes: evidence for an intrinsic pancreatic alpha cell defect. *Science* 182: 171–173, 1973.
12. **Gopel SO, Kanno T, Barg S, Weng XG, Gromada J, and Rorsman P.** Regulation of glucagon release in mouse α-cells by K_{ATP} channels and inactivation of TTX-sensitive Na^+ channels. *J Physiol* 528: 509–520, 2000.
13. **Greenbaum CJ, Havel PJ, Taborsky GJ Jr, and Klaff LJ.** Intra-islet insulin permits glucose to directly suppress pancreatic A cell function. *J Clin Invest* 88: 767–773, 1991.
14. **Greenbaum CJ, Progeon RL, and D'Alessio DA.** Impaired β-cell function, incretin effect, and glucagon suppression in patients with type 1 diabetes who have normal fasting glucose. *Diabetes* 51: 951–957, 2002.
15. **Gromada J, Bokvist K, Ding WG, Barg S, Buschard K, Renstrom E, and Rorsman P.** Adrenalin stimulates glucagon secretion in pancreatic A-cells by increasing the Ca2+ current and the number of granules close to the L-type Ca channels. *J Gen Physiol* 100: 217–228, 1997.
16. **Gromada J, Ma X, Hoy M, Bokvist K, Salehi A, Berggren PO, and Rorsman P.** ATP-sensitive K^+ channel-dependent regulation of glucagon release and electrical activity by glucose in wild-type and $SUR1^{-/-}$ mouse α-cells. *Diabetes* 53, *Suppl* 3: S181–S189, 2004.
17. **Ishihara H, Maechler P, Gjinovci A, Herrera PL, and Wollheim CB.** Islet β-cell secretion determines glucagon secretion from the neighboring α-cells. *Nat Cell Biol* 5: 330–335, 2003.
18. **Ishihara H, Wang H, Drewes LR, and Wollheim CB.** Overexpression of monocarboxylate transporter and lactate dehydrogenase alters insulin secretory responses to pyruvate and lactate in β-cells. *J Clin Invest* 104: 1621–1629, 1999.
19. **Iwashima Y, Watanabe K, Eto M, Morikawa A, Takebe T, and Ishii K.** Insulin and glucagon response of the diabetic Chinese hamster in the Asahikawa colony. *Diabetes Res Clin Pract* 1: 87–94, 1985.
20. **Juhl K and Hutton J.** Stimulus-secretion coupling in the pancreatic β-cell. *Adv Exp Med Biol* 552: 66–90, 2004.
21. **Khan FA, Goforth PB, Zhang M, and Satin LS.** Insulin activates ATP-sensitive K(+) channels in pancreatic beta-cells through a phosphatidylinositol 3-kinase-dependent pathway. *Diabetes* 50: 2192–2198, 2001.
22. **Lantz KA, Vatamaniuk MZ, Brestelli JE, Friedman JR, Matschinsky FM, and Kaestner KH.** Foxa2 regulates multiple pathways of insulin secretion. *J Clin Invest* 114: 512–520, 2004.
23. **Liu YJ, Vieira E, and Gylfe E.** A store-operated mechanism determines the activity of the electrically excitable glucagon-secreting α-cell. *Cell Calcium* 35: 357–365, 2004.
24. **MacDonald MJ and Fahien LA.** Glyceraldehyde phosphate and methyl esters of succinic acid. Two "new" potent insulin secretagogues. *Diabetes* 37: 997–999, 1988.
25. **Merglen A, Theander S, Rubi B, Chaffard G, Wollheim CB, and Maechler P.** Glucose sensitivity and metabolism-secretion coupling studied during two-year continuous culture in INS-1E insulinoma cells. *Endocrinology* 145: 667–678, 2004.
26. **Miki T, Liss B, Minami K, Shiuchi T, Saraya A, Kashima Y, Horiuchi M, Ashcroft F, Minokoshi Y, Roeper J, and Seino S.** ATP-sensitive K+ channels in the hypothalamus are essential for the maintenance of glucose homeostasis. *Nat Neurosci* 4: 507–512, 2001.
27. **Miyake S, Makimura M, Kanegae Y, Harada S, Sato Y, Takamori K, Tokuda C, and Saito I.** Efficient generation of recombinant adenoviruses using adenovirus DNA-terminal protein complex and a cosmid bearing the full-length virus genome. *Proc Natl Acad Sci USA* 93: 1320–1324, 1996.
28. **Niwa H, Yamamura K, and Miyazaki J.** Efficient selection for high-expression transfectants with a novel eukaryotic vector. *Gene* 108: 193–199, 1991.
29. **Noel RJ, Antinozzi PA, McGarry D, and Newgard CB.** Engineering of glycerol-stimulated insulin secretion in islet β-cells. *J Biol Chem* 272: 18621–18627, 1997.
30. **Oetergard T, Degn KB, Gall MA, Carr RD, Veldhouis JD, Thomsen MK, Rizza RA, and Schmitz O.** The insulin secretagogues glibenclamide and repaglinide do not influence growth hormone secretion in humans but stimulate glucagon secretion during insulin deficiency. *J Clin Endocrinol Metab* 89: 297–302, 2004.
31. **Okamoto K, Hirano H, and Isohashi F.** Molecular cloning of rat liver glucocorticoid-receptor translocation promoter. *Biochem Biophys Res Commun* 193: 848–854, 1993.
32. **Pipeleers DG, Schuit FC, Van Schravendijk CFH, and Van de Winkel M.** Interplay of nutrients and hormones in the regulation of glucagon release. *Endocrinology* 117: 817–823, 1985.

33. **Ravier MA and Rutter GA.** Glucose or insulin, but not zinc ions, inhibit glucagon secretion from mouse pancreatic α-cells. *Diabetes* 54: 1789–1797, 2005.
34. **Schuit F, Derde MP, and Pipelers D.** Sensitivity of rat pancreatic A and B cell to somatostatin. *Diabetologia* 32: 207–212, 1989.
35. **Schuit F, DeVos A, Farfari S, Moens K, Pipelers D, Brun T, and Prentki M.** Metabolic fate of glucose in purified islet cells. *J Biol Chem* 272: 18572–18579, 1997.
36. **Sekine T, Cha SH, Hosoyamada M, Kanai Y, Watanabe N, Furuta Y, Fukuda K, Igarashi T, and Endou H.** Cloning, functional characterization, and localization of a rat renal Na^+-dicarboxylate transporter. *Am J Physiol Renal Physiol* 275: F298–F305, 1998.
37. **Taborsky GJ Jr, Ahren B, and Havel PJ.** Autonomic mediation of glucagon secretion during hypoglycemia: implications for impaired α-cell responses in type 1 diabetes. *Diabetes* 47: 995–1005, 1998.
38. **The Diabetes Control, and Complications Trial Research Group.** The effect of intensive treatment of diabetes on the development and progression of long-term complications in insulin-dependent diabetes mellitus. *N Engl J Med* 329: 977–986, 1993.
39. **Wendt A, Birnir B, Buschard K, Gromada J, Salehi A, Sewing S, Rorsman P, and Braun M.** Glucose inhibition of glucagon secretion from rat α-cells is mediated by GABA released from neighboring β-cells. *Diabetes* 53: 1038–1045, 2004.

Signals from intra-abdominal fat modulate insulin and leptin sensitivity through different mechanisms: Neuronal involvement in food-intake regulation

Tetsuya Yamada,[1,7] Hideki Katagiri,[2,7,*] Yasushi Ishigaki,[1,7] Takehide Ogihara,[2] Junta Imai,[1,2] Kenji Uno,[1,2] Yutaka Hasegawa,[1,2] Junhong Gao,[1,2] Hisamitsu Ishihara,[1] Akira Niijima,[3] Hiroyuki Mano,[4] Hiroyuki Aburatani,[5] Tomoichiro Asano,[6] and Yoshitomo Oka[1]

[1]Division of Molecular Metabolism and Diabetes
[2]Division of Advanced Therapeutics for Metabolic Diseases, Center for Translational and Advanced Animal Research
Tohoku University Graduate School of Medicine, Sendai 980-8575, Japan
[3]Niigata University School of Medicine, Niigata 951-8150, Japan
[4]Division of Functional Genomics, Jichi Medical School, Kawachi-gun, Tochigi 329-0498, Japan
[5]Research Center for Advanced Science and Technology, University of Tokyo, Tokyo 153-8904, Japan
[6]Department of Physiological Chemistry and Metabolism, University of Tokyo, Tokyo 113-8655, Japan
[7]These authors contributed equally to this work.
*Correspondence: katagiri-tky@umin.ac.jp

Summary

Intra-abdominal fat accumulation is involved in development of the metabolic syndrome, which is associated with insulin and leptin resistance. We show here that ectopic expression of very low levels of uncoupling protein 1 (UCP1) in epididymal fat (Epi) reverses both insulin and leptin resistance. UCP1 expression in Epi improved glucose tolerance and decreased food intake in both diet-induced and genetically obese mouse models. In contrast, UCP1 expression in Epi of leptin-receptor mutant mice did not alter food intake, though it significantly decreased blood glucose and insulin levels. Thus, hypophagia induction requires a leptin signal, while the improved insulin sensitivity appears to be leptin independent. In wild-type mice, local-nerve dissection in the epididymis or pharmacological afferent blockade blunted the decrease in food intake, suggesting that afferent-nerve signals from intra-abdominal fat tissue regulate food intake by modulating hypothalamic leptin sensitivity. These novel signals are potential therapeutic targets for the metabolic syndrome.

Introduction

The explosive increase in obesity has become a major public health concern in most industrialized countries (Flier, 2004; Friedman, 2003). Insulin resistance is a fundamental contributor to the metabolic syndrome associated with type 2 diabetes, hypertension, hyperlipidemia, and atherosclerosis. Major advancements in this field include the discoveries of adipocyte-derived humoral factors, such as leptin (Friedman and Halaas, 1998). Leptin conveys energy-storage information from adipose tissue to the central nervous system, leading to food-intake suppression. However, in patients with ordinary obesity, serum leptin levels are increased in proportion to body fat (Considine et al., 1996), but the responses to leptin are impaired (Heymsfield et al., 1999), which defines a state of leptin resistance. Leptin resistance also contributes to the development of obesity and obesity-related metabolic disorders.

Fat accumulation in intra-abdominal fat tissue is involved in development of the metabolic syndrome (Bjorntorp, 1992; Matsuzawa et al., 1995) associated with insulin and leptin resistance (Friedman, 2003). Therefore, in this study, to examine whether the metabolic changes in intra-abdominal fat tissue affect insulin and leptin resistance as well as systemic glucose metabolism, we attempted to express uncoupling protein 1 (UCP1), which functions to dissipate energy as heat (Klingenberg and Huang, 1999), in epididymal fat tissue (Epi) in mice with obesity and diabetes.

Results and discussion

C57BL/6 mice were subjected to direct injection of the UCP1 adenovirus vector into Epi (UCP1 mice) after the development of diabetes associated with obesity in response to high-fat chow preloading for 4 weeks. Mice given the LacZ adenovirus were used as controls (LacZ mice). Immunoblotting detected adenovirus-mediated UCP1 expression in Epi (see Figure S1A in the Supplemental Data available with this article online), and this expression was restricted to Epi (Fig. S1A). UCP1 expression in Epi was detectable on the first day after adenoviral injection and was increased on day 3 but had fallen to very low levels by day 7 (Figure S1B). However, expression levels were far below those of endogenous protein in BAT: on day 3, approximately 5% per unit weight protein (Figure S1B). UCP1 expression was restricted to very limited portions of the tissue (left panel of Figure 1B). Judging from the intensity of immunostaining, UCP1 expression levels in UCP1-expressing white adipocytes did not reach those in brown adipocytes (right panel of Figure 1B). UCP1-expressing adipocytes were significantly smaller than UCP1-nonexpressing adipocytes in the same tissue (Figure 1C), suggesting enhanced metabolism in the former.